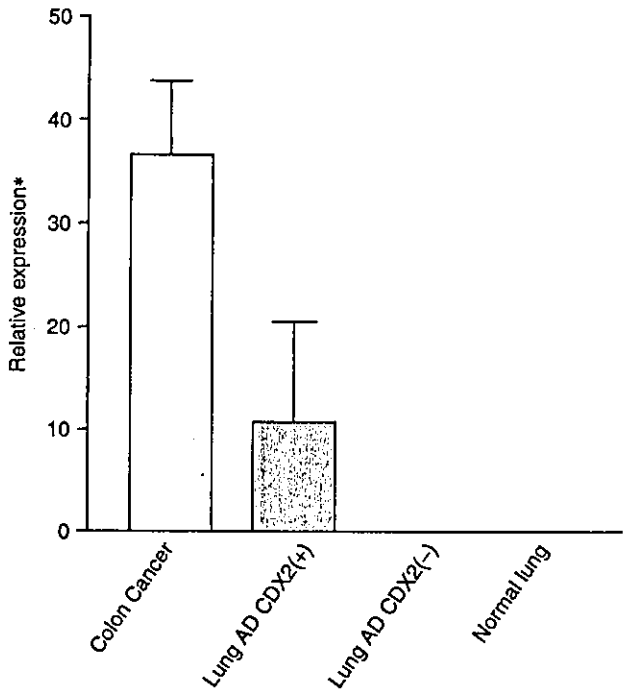

Samples	n=	Average	SEM
Colon cancer	3	36.6	7.1
Normal lung	3	0.0	0.0
Lung AD, CDX2(+)	5	10.7	9.7
Lung AD, CDX2(–)	5	0.0	0.0

* Relative to expression of HT29; SEM, standard error of the mean

Figure 3. Expression of CDX2 transcripts in colon, normal lung, and lung cancers. CDX2 transcript levels correlated well with protein expression, evaluated by immunohistochemistry

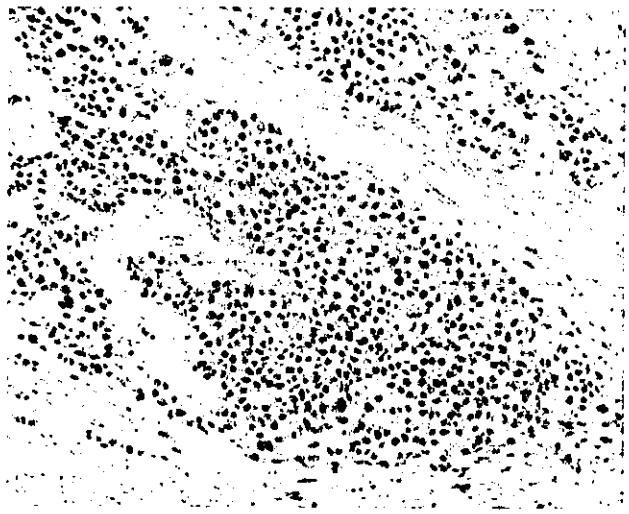

Score	n=	0	1+	2+	3+	4+
TC	6	6	0	0	0	0
AC	2	1	0	1	0	0
LCNEC	8	5	1	0	2	0
SCLC	16	13	2	0	1	0

TC, typical carcinoid; AC, atypical carcinoid;
LCNEC, large cell neuroendocrine carcinoma;
SCLC, small cell lung cancer

Figure 4. CDX2 expression in a spectrum of pulmonary neuroendocrine tumours. Most of the CDX2-positive tumours were high-grade neuroendocrine tumours (large cell neuroendocrine tumors and small cell lung cancers). Six of the 24 tumours (25%) were positive for CDX2. A representative picture scoring 3+ is shown in the upper panel

tissue-specific expression of TTF-1 [30] and MGB1 (unpublished observations) in peripheral lung and breast, respectively. Unexpectedly, both molecules were expressed in pulmonary high-grade neuroendocrine carcinomas. Similar findings were obtained by others [31,32]. Furthermore, ectopic expression of c-kit and the stem cell factor is common in small cell lung carcinomas [33,34]. We suspect that aberrant expression of these molecules is related to the nature of this tumour, which is characterized by its undifferentiated or primitive morphology. Shamblott *et al* reported that human pluripotent stem cells derived from primordial germ cells simultaneously express markers of neural, vascular, haematopoietic, muscle, and endodermal lineages [35]. This is not an artefact of culture conditions, because Akashi *et al* have reported similar multi-lineage expression in haematopoietic stem cells, which were freshly prepared using Dynabeads and a fluorescence-activated cell sorter [36]. Expression of lineage-specific molecules in pulmonary high-grade neuroendocrine tumours may have some association with the multi-lineage gene expression of stem cells.

The frequency of *K-ras* mutation in the present study (14%) appeared to be low compared with that of pervious studies, in which the mutation was detected in about 30–40% of lung adenocarcinomas. This low frequency is not due to our RNA-based analysis, because *p53* mutation was detected with a prevalence similar to previous studies using the same methods and the same RNA samples (data not shown). There may be ethnic or geographical differences in the prevalence of *K-ras* mutation, because Hunt *et al* reported an increased prevalence of the mutation in African-Americans around the Mississippi river [37], and a low frequency of *K-ras* mutation in Japanese subjects has been reported previously by us [38] and in other Japanese studies [3,39].

In summary, we have demonstrated that there is a subset of lung adenocarcinomas that frequently show expression of CK20 and CDX2, *K-ras* mutations, and/or goblet cell morphology. These phenotypes are commonly observed in other organs, suggesting that adenocarcinomas with these features are one of the prototypes that are independent of the organ of origin. The study also calls the attention of surgical pathologists to CDX2 expression in lung adenocarcinomas. Whereas CDX2 expression is very high and uniform in colorectal carcinomas, as reported previously, some lung adenocarcinomas may express CDX2. In this case, CK20 also tends to be positive, so that the differential diagnosis should be integrated with other findings. In addition to lung adenocarcinomas, pulmonary high-grade neuroendocrine tumours may also be positive for CDX2.

Acknowledgements

We thank Kaori Hayashi for excellent technical assistance with the molecular genetic experiments and Hiroji Ishida for assistance in constructing the tissue array.

References

1. Shimosato Y. Lung tumors. In *Diagnostic Surgical Pathology* (3rd edn), Sternberg SS, Antonioli DA, Carter D, Mills SE, Oberman HA, Sinard JH (eds). Lippincott Williams & Wilkins: Philadelphia, 1999.
2. Kobayashi T, Tsuda H, Noguchi M, *et al.* Association of point mutation in c-Ki-ras oncogene in lung adenocarcinoma with particular reference to cytologic subtypes. *Cancer* 1990; **66**: 289–294.
3. Tsuchiya E, Furuta R, Wada N, *et al.* High K-ras mutation rates in goblet-cell-type adenocarcinomas of the lungs. *J Cancer Res Clin Oncol* 1995; **121**: 577–581.
4. Marchetti A, Buttitta F, Pellegrini S, *et al.* Bronchioloalveolar lung carcinomas: K-ras mutations are constant events in the mucinous subtype. *J Pathol* 1996; **179**: 254–259.
5. Miettinen M. Keratin 20: immunohistochemical marker for gastrointestinal, urothelial, and Merkel cell carcinomas. *Mod Pathol* 1995; **8**: 384–388.
6. Di Loreto C, Di Lauro V, Puglisi F, Damante G, Fabbro D, Beltrami CA. Immunocytochemical expression of tissue specific transcription factor-1 in lung carcinoma. *J Clin Pathol* 1997; **50**: 30–32.
7. Cai YC, Banner B, Glickman J, Odze RD. Cytokeratin 7 and 20 and thyroid transcription factor 1 can help distinguish pulmonary from gastrointestinal carcinoid and pancreatic endocrine tumors. *Hum Pathol* 2001; **32**: 1087–1093.
8. Lau SK, Desrochers MJ, Luthringer DJ. Expression of thyroid transcription factor-1, cytokeratin 7, and cytokeratin 20 in bronchioloalveolar carcinomas: an immunohistochemical evaluation of 67 cases. *Mod Pathol* 2002; **15**: 538–542.
9. Chu PG, Weiss LM. Keratin expression in human tissues and neoplasms. *Histopathology* 2002; **40**: 403–439.
10. Chu P, Wu E, Weiss LM. Cytokeratin 7 and cytokeratin 20 expression in epithelial neoplasms: a survey of 435 cases. *Mod Pathol* 2000; **13**: 962–972.
11. Shah RN, Badve S, Papreddy K, Schindler S, Laskin WB, Yeldandi AV. Expression of cytokeratin 20 in mucinous bronchioloalveolar carcinoma. *Hum Pathol* 2002; **33**: 915–920.
12. Goldstein NS, Thomas M. Mucinous and nonmucinous bronchioloalveolar adenocarcinomas have distinct staining patterns with thyroid transcription factor and cytokeratin 20 antibodies. *Am J Clin Pathol* 2001; **116**: 319–325.
13. Yuasa Y. Control of gut differentiation and intestinal-type gastric carcinogenesis. *Nature Rev Cancer* 2003; **3**: 592–600.
14. Suh E, Traber PG. An intestine-specific homeobox gene regulates proliferation and differentiation. *Mol Cell Biol* 1996; **16**: 619–625.
15. Moskaluk CA, Zhang H, Powell SM, Cerilli LA, Hampton GM, Frierson HF. Cdx2 protein expression in normal and malignant human tissues: an immunohistochemical survey using tissue microarrays. *Mod Pathol* 2003; **16**: 913–919.
16. Barbareschi M, Murer B, Colby TV, *et al.* CDX-2 homeobox gene expression is a reliable marker of colorectal adenocarcinoma metastases to the lungs. *Am J Surg Pathol* 2003; **27**: 141–149.
17. Greene FL, Page DL, Fleming ID, *et al* (eds). *AJCC Cancer Staging Manual* (6th edn). Springer-Verlag: New York, 2002.
18. Yatabe Y. Role of expression of thyroid transcription factor-1 in pulmonary adenocarcinoma. In *Immunohistochemistry and In Situ Hybridization of Human Carcinomas*, Hayat MA (ed). Elsevier Science/Academic Press: New York, in press.
19. Yatabe Y, Osada H, Tatematsu Y, Mitsudomi T, Takahashi T. Decreased expression of 14-3-3 sigma in neuroendocrine tumors is independent of origin and malignant potential. *Oncogene* 2002; **21**: 8310–8319.
20. Bos JL. ras oncogenes in human cancer: a review. *Cancer Res* 1989; **49**: 4682–4689.
21. Mitsudomi T, Viallet J, Mulshine JL, Linnoila RI, Minna JD, Gazdar AF. Mutations of ras genes distinguish a subset of non-small-cell lung cancer cell lines from small-cell lung cancer cell lines. *Oncogene* 1991; **6**: 1353–1362.
22. Werling RW, Yaziji H, Bacchi CE, Gown AM. CDX2, a highly sensitive and specific marker of adenocarcinomas of intestinal origin. An immunohistochemical survey of 376 primary and metastatic carcinomas. *Am J Surg Pathol* 2003; **27**: 303–310.
23. Ichikawa Y, Nishida M, Suzuki H, *et al.* Mutation of K-ras protooncogene is associated with histological subtypes in human mucinous ovarian tumors. *Cancer Res* 1994; **54**: 33–35.
24. Johnson RL, Rothman AL, Xie J, *et al.* Human homolog of patched, a candidate gene for the basal cell nevus syndrome. *Science* 1996; **272**: 1668–1671.
25. Bignell GR, Warren W, Seal S, *et al.* Identification of the familial cylindromatosis tumour-suppressor gene. *Nature Genet* 2000; **25**: 160–165.
26. Brown K, Strathdee D, Bryson S, Lambie W, Balmain A. The malignant capacity of skin tumours induced by expression of a mutant H-ras transgene depends on the cell type targeted. *Curr Biol* 1998; **8**: 516–524.
27. Grachtchouk M, Mo R, Yu S, *et al.* Basal cell carcinomas in mice overexpressing Gli2 in skin. *Nature Genet* 2000; **24**: 216–217.
28. Gat U, DasGupta R, Degenstein L, Fuchs E. *De novo* hair follicle morphogenesis and hair tumors in mice expressing a truncated beta-catenin in skin. *Cell* 1998; **95**: 605–614.
29. Franchi A, Massi D, Baroni G, Santucci M. CDX-2 homeobox gene expression (Letter). *Am J Surg Pathol* 2003; **27**: 1390–1391.
30. Yatabe Y, Mitsudomi T, Takahashi T. TTF-1 expression in pulmonary adenocarcinomas. *Am J Surg Pathol* 2002; **26**: 767–773.
31. Sturm N, Rossi G, Lantuejoul S, *et al.* Expression of thyroid transcription factor-1 in the spectrum of neuroendocrine cell lung proliferations with special interest in carcinoids. *Hum Pathol* 2002; **33**: 175–182.
32. Wu M, Wang B, Gil J, *et al.* p63 and TTF-1 immunostaining. A useful marker panel for distinguishing small cell carcinoma of lung from poorly differentiated squamous cell carcinoma of lung. *Am J Clin Pathol* 2003; **119**: 696–702.
33. Hibi K, Takahashi T, Sekido Y, *et al.* Coexpression of the stem cell factor and the c-kit genes in small-cell lung cancer. *Oncogene* 1991; **6**: 2291–2296.
34. Sekido Y, Obata Y, Ueda R, *et al.* Preferential expression of c-kit protooncogene transcripts in small cell lung cancer. *Cancer Res* 1991; **51**: 2416–2419.
35. Shamblott MJ, Axelman J, Littlefield JW, *et al.* Human embryonic germ cell derivatives express a broad range of developmentally distinct markers and proliferate extensively *in vitro*. *Proc Natl Acad Sci U S A* 2001; **98**: 113–118.
36. Akashi K, He X, Chen J, *et al.* Transcriptional accessibility for genes of multiple tissues and hematopoietic lineages is hierarchically controlled during early hematopoiesis. *Blood* 2003; **101**: 383–389.
37. Hunt JD, Strimas A, Martin JE, *et al.* Differences in KRAS mutation spectrum in lung cancer cases between African Americans and Caucasians after occupational or environmental exposure to known carcinogens. *Cancer Epidemiol Biomarkers Prev* 2002; **11**: 1405–1412.
38. Endoh H, Yatabe Y, Shimizu S, *et al.* RASSF1A gene inactivation in non-small cell lung cancer and its clinical implication. *Int J Cancer* 2003; **106**: 45–51.
39. Huang CL, Taki T, Adachi M, *et al.* Mutations of p53 and K-ras genes as prognostic factors for non-small cell lung cancer. *Int J Oncol* 1998; **12**: 553–563.

Oncogene (2004) 23, 4041–4049

www.nature.com/onc

ORIGINAL PAPERS

Maspin expression in normal lung and non-small-cell lung cancers: cellular property-associated expression under the control of promoter DNA methylation

Yasushi Yatabe[1,*], Tetsuya Mitsudomi[2] and Takashi Takahashi[3]

[1]*Department of Pathology and Molecular Diagnostics, Aichi Cancer Center Hospital, Nagoya, Japan;* [2]*Department of Thoracic Surgery, Aichi Cancer Center Hospital, Nagoya, Japan;* [3]*Division of Molecular Oncology, Aichi Cancer Center Research Institute, Nagoya, Japan*

Maspin has been demonstrated to be a suppressor of invasion and cell motility *in vitro*, whereas *in vivo* analyses have reported that increased expression of maspin is associated with malignant behavior. The present study examined maspin expression in normal lung and non-small-cell lung cancers. Only proximal airway cells in the normal lung expressed maspin, and the expression was associated with decreased methylation. This association was also observed in non-small-cell lung cancers, but the expression was quite different among histologic subtypes; 20 of 21 squamous cell carcinomas showed intense, uniform expression, whereas the expression status varied among adenocarcinomas. Of the 119 adenocarcinomas, 60 were negative, 23 positive and 36 showed a heterogeneous expression pattern. The expression was inversely correlated with markers of peripheral airway cells. Taken together, the results suggest that maspin may be expressed in association with the proximal airway cell type. It is of note that the heterogeneous expression pattern of maspin is quite distinctive, showing geographic positivity in the individual tumors. Separate analysis of methylation status in positive and negative portions of individual tumors provided an instance of intratumor diversity associated with promoter DNA methylation.
Oncogene (2004) **23**, 4041–4049. doi:10.1038/sj.onc.1207557
Published online 29 March 2004

Keywords: maspin; non-small-cell lung cancers; intratumor heterogeneity; promoter DNA methylation; cellular properties

Introduction

The mammary serine protease inhibitor maspin was first isolated by Zou *et al.* (1994) as a defective molecule in breast carcinoma cells by differential display analysis. Maspin exhibits significant homology to the serpin superfamily of serine protease inhibitors, which includes the plasminogen activator inhibitors 1 and 2 (PAI-1 and PAI-2), and α1-antitrypsin. Recent analyses *in vitro* have suggested an inhibitory effect on tumor invasion and metastasis. Cell motility and invasion are inhibited with transfection of the maspin gene into cancer cell lines, and the transplantation of the transfectants in nude mice led to reduced tumorgenicity and decreased metastatic potential (Sheng *et al.*, 1994; Zou *et al.*, 1994; Sheng *et al.*, 1996; Zou *et al.*, 2000). The mechanism underlying maspin's inhibitory activity remains controversial, but recent reports suggested that it does not directly inhibit matrix-degrading proteases, but rather functions as a regulator of plasminogen-tissue-type plasminogen activator complex (Bass *et al.*, 2002). On the other hand, it has been shown that maspin has two consensus p53-binding sequences in its promoter region, and p53 regulated maspin expression, indicating that maspin is one of the target genes of p53 pathway (Zou *et al.*, 2000). Furthermore, maspin was shown to have an inhibitory effect on tumor angiogenesis (Zhang *et al.*, 2000) and a sensitizing effect on apoptosis (Jiang *et al.*, 2002). Despite a tumor suppressing role *in vitro*, clinicopathological analysis using *in vivo* tumors failed to demonstrate the role, and maspin-expressing tumors tend to show more malignant behavior, including shorter survivals, in breast cancers (Umekita *et al.*, 2002; Bieche *et al.*, 2003), pancreatic cancers (Maass *et al.*, 2001) and ovarian cancers (Sood *et al.*, 2002).

Promoter DNA hypermethylation is one of the epigenetic mechanisms to silence certain genes. So far, a number of genes have been shown to be inactivated by this gene silencing (Jones and Baylin, 2002; Laird, 2003), whereas the silencing was predominantly reported in the cancer tissues, but not in normal tissues. Although the involvement of DNA methylation in X-chromosome inactivation (Mohandas *et al.*, 1981) and genomic imprinting (Li *et al.*, 1993) has been widely accepted, tissue-specific regulation of gene expression in normal tissues mediated by DNA methylation has long been speculated. Recently, Futscher *et al.* (2002) first demonstrated that the tissue-specific expression of maspin was

*Correspondence: Y Yatabe, Department of Pathology and Molecular Diagnostics, Aichi Cancer Center Hospital, Kanokoden, Chikusa-ku, Nagoya 464-8681, Japan; E-mail: yyatabe@aichi-cc.jp
Received 1 October 2003; revised 25 December 2003; accepted 20 January 2004; Published online 29 March 2004

controlled by DNA methylation. They described a close correlation between maspin expression and the absence of DNA methylation using various normal tissues, and this expression in immortalized cells was restored by treatment with 5-aza-2′-deoxycytidine. In addition to normal tissues, the gene silencing of maspin was observed in breast cancers (Domann *et al*., 2000; Maass *et al*., 2002), suggesting a contribution to breast carcinogenesis.

Lung cancers, especially adenocarcinomas, are characterized by a high degree of morphological heterogeneity, which in turn implies both intra- and intertumor diversities. We have been interested in and have analysed the diversities. Recently, we revealed that thyroid transcription factor-1, TTF-1, serves as a lineage marker for peripheral airway cells, including type I and II pneumocytes (Yatabe *et al*., 2002). Furthermore, analysis of various cancer-associated genes, including p53 (Nishio *et al*., 1997), cyclin D1 (Nishio *et al*., 1997), RB (Nishio *et al*., 1997), $p27^{Kip1}$ (Yatabe *et al*., 1998b) and COX1 (Yatabe *et al*., 1998a; Achiwa *et al*., 1999), suggests a different molecular pathway for carcinogenesis in lung adenocarcinomas between cells with and without TTF-1 expression. This result implies that one of the intertumor heterogeneities of lung adenocarcinoma is represented by putative original cells, that is, peripheral airway cell-derived carcinomas and the others. This distinction is supported by the expression profiling analysis (Bhattacharjee *et al*., 2001; Garber *et al*., 2001). Unsupervised hierarchical clustering, based on the molecular signature, classified lung adenocarcinomas largely into two subtypes, which were delineated by TTF-1. The present study also focused on the diversities. First, we confirmed cell-type-specific expression of maspin, and then we examined lung tumors, revealing that maspin is expressed in a highly heterogeneous fashion in lung adenocarcinomas, similar to the morphology. We found that the expression of maspin is associated with cell type in lung tissue, while intratumor diversity of maspin is associated with regional promoter hypermethylation. There are few references in the literature concerning DNA methylation associated with the intratumor diversity (Graff *et al*., 2000; Nass *et al*., 2000; Markl *et al*., 2001), and this study therefore provides new information regarding maspin expression, which might shed light on the complex mechanism of the metastatic process.

Results

Cell-type-specific expression of maspin in the normal lung

Tissue-specific expression, including airway epithelium, has been previously reported (Futscher *et al*., 2002), but there are various types of the epithelium covering airway tracts. Therefore, we further examined which cell types in the airway epithelium expressed maspin. Immunohistochemical analysis demonstrated a characteristic expression pattern, and this expression was restricted to the basal cells of the bronchial epithelium (Figure 1 (a1)) and myoepithelium of the bronchial glandular acini (Figure 1 (a2)). This was in sharp contrast to the peripheral portion of the lung parenchyma; none of the cells in the peripheral lung, such as type I and II pneumocytes, were positive for maspin (Figure 1 (a4)). In the bronchiolar cells that connect the bronchus to the peripheral lung, a number of maspin-expressing cells were decreased (Figure 1 (a3)).

Figure 1 Maspin expression in normal lung tissue (**a**) from a proximal airway (a1) to peripheral lung parenchyma (a4). Basal cells of the bronchial surface epithelium (a1), and myoepithelium of the bronchial glands (a2), expressed maspin. Positive signal frequency was reduced as being close to the alveolar spaces (bronchioles, A3), and no expression was detected in the alveolar spaces (a4). Squamous cell carcinoma (**b**) demonstrates intense, uniform expression, whereas the expression was varied among adenocarcinomas. A similar positive pattern was seen in mucinous bronchioloalveolar carcinoma (**c**). However, an ordinary peripheral type of adenocarcinoma is completely negative for maspin despite the positive internal control for bronchial epithelium (**d**)

Maspin expression in lung cancers

Similar to the normal lung, a cell-type-specific pattern of maspin expression was observed in non-small-cell lung cancers (Table 1). All of the squamous cell carcinomas, except a single case, expressed maspin intensively and very uniformly (Figure 1b), whereas adenocarcinomas demonstrated a variety of expression patterns (Figure 1c and d). Of the 119 adenocarcinomas, 60 (50.4%) were negative for maspin, while 23 (19.3%) demonstrated a uniform, and 36 (30.3%) a heterogeneous expression pattern for maspin. The heterogeneous expression pattern of maspin was quite distinctive, and details are discussed later.

Columnar cell-specific expression in normal lung tissue prompted us to explore the biological significance of maspin expression in pulmonary adenocarcinomas. First, we examined the clinicopathological characteristics of the maspin-positive adenocarcinoma, which is summarized in Table 2. Although maspin expression was not associated with sex, smoking status or

pathological stage, maspin expression was more frequently observed in advanced local tumor status (pT). In the scheme of lung cancer staging classification, pT is determined by tumor size and an extent of local invasion. Individual analysis of tumor size and local invasiveness revealed that the correlation of maspin expression with pT was primarily dependent on the prevalence of maspin expression in larger tumors, but not that of locally invasive tumors. In addition, the presence of lymph node metastasis was independent of maspin expression.

We have recently proposed the subclassification of lung adenocarcinoma into two major subtypes of peripheral airway adenocarcinoma and the remainder, which are delimited by TTF-1. Interestingly, maspin expression is inversely correlated with TTF-1 expression, being consistent with proximal airway-specific expression of maspin in the normal lung. This was confirmed by the expression status of surfactant precursor protein B, which is known as a differentiation marker for pneumocytes. p53 alteration is frequent in maspin-expressing adenocarcinomas, and is also consistent with less-frequent p53 alteration in TTF-1-positive adenocarcinomas. Therefore, this suggests that maspin is expressed in association with cellular type of the nonperipheral airway epithelium even after malignant transformation. Selective expression of maspin in normal proximal airway cells suggests that maspin may be expressed in association with proximal airway cell type. The K-*ras* mutation is also prevalent in maspin-expressing adenocarcinomas.

Table 1 Maspin expression of non-small-cell lung cancers

	Maspin expression		
	Mostly negative	*Heterogeneous*	*Mostly positive*
Adenocarcinoma	60	36	23
Squamous cell carcinoma	0	1	20
Large cell carcinoma	0	1	2
Adenosquamous ca.	0	0	1

Heterogeneous expression of maspin in lung cancers

During the examination, we found that the heterogeneous pattern of maspin expression was distinct from the common expression pattern; the expression pattern was very geographic, that is, a part of the tumor intensely expressed maspin, but the other was completely negative (Figure 2). In 36 of the 119 adenocarcinoma cases examined, maspin expression varied among the tissue-microarrayed cores in individual tumors. Therefore, we further analysed with regular whole sections, and confirmed the geographic expression of maspin in 36 adenocarcinoma cases. This heterogeneous expression appears to be inconsistent with the idea of proximal airway-cell-type-associated expression of maspin, because characteristic uniform expression of TTF-1 was observed in 25 of 36 adenocarcinomas with heterogeneous maspin expression (Table 2). On this matter, following two points were addressed. First, we examined the expression status of maspin in preneoplastic lesions and *in situ* carcinoma of a peripheral type of adenocarcinoma. All five atypical adenomatous hyperplasia and five nonmucinous bronchioloalveolar carcinomas (carcinoma *in situ*) were positive for TTF-1, but negative for maspin. Second, clinicopathological characteristics of the heterogeneous expression among the TTF-1-positive, peripheral airway cell-associated adenocarcinomas were examined. Heterogeneous expression was associated with higher histologic grade (χ^2 test, $P=0.02$) and lower frequency of surfactant expression (Fisher's exact test, $P=0.03$), suggesting that maspin heterogeneity was prevalent in less-differentiated tumors in the category of peripheral airway cell-associated adenocarcinomas. These findings imply that maspin should be considered as a differentiation marker rather than a lineage marker.

Characteristics of maspin-positive portions in the individual tumors were then analysed. Although there was some unexpected expression, two morphologically characteristic portions tended to be positive for maspin: a portion showing solid growth pattern (Figure 2b), and a portion with infiltrating cancer cells in small clusters (Figure 2d). Some adenocarcinomas contained either solid or infiltrating patterns, while the other

Table 2 Clinicopathologic features of adenocarcinoma in relation to maspin expression

	Maspin expression			
	Negative	*Heterogeneous*	*Positive*	P-*value*
n	60	36	23	
Female/male	35/25	16/20	11/12	0.38
Smoker/nonsmoker	33/27	16/20	7/16	0.12
pStage (Stage I/>Stage I)	40/20	18/18	15/8	1.00
pT1/>pT1	32/28	10/26	7/16	0.02
Size ⩽30 mm/>30 mm	44/16	18/18	9/14	<0.01
Local pleural invasion	41/19	19/17	16/17	0.25
pN0/>pN0	41/19	23/13	19/4	0.30
TTF-1 +/−	52/8	25/11	4/19	<0.01
SPPB +/−	46/14	16/20	4/19	<0.01
p53 wild type/mutated	38/18	25/10	8/13	0.03
K-*ras* wild type/mutated	53/2	32/3	15/6	<0.01

simultaneously had both patterns. It is of note, however, that maspin expression was not always associated with these features of tumor growth, in that not all of the invasive portions and/or solid portions were positive for maspin (Figure 3). The portions with and without the expression were morphologically indistinguishable. The findings raised a question about which portion was associated with metastasis. We therefore compared the expression pattern between primary and metastatic sites in order to ascertain the role of maspin in metastasis. Of the 36 adenocarcinomas with heterogeneous expression, 13 tumors metastasized to the lymph nodes, with only 12 able to be examined. The results are summarized in Figure 3, and the expression status in half of the 12 tumors was decreased compared to that of the corresponding lymph nodes.

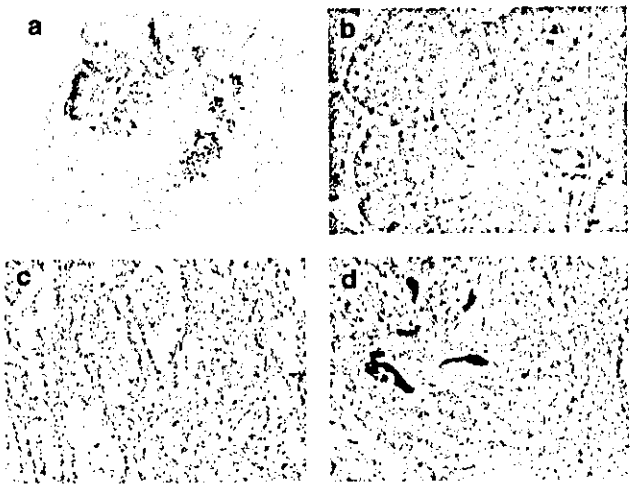

Figure 2 (a) Representative case with heterogeneous expression of maspin. Gross appearance demonstrates a characteristic geographic pattern of expression (a). The solid growth area shows intense, uniform positivity for maspin (b) and the tubular growth area is completely negative (c). In part, infiltrating cancer cells in small clusters are intensely positive for maspin (d)

Maspin expression associated with promoter DNA methylation

The relationship between the expression and methylation status was examined in lung cancer cell lines. The promoter region of the maspin gene was densely methylated in five of 13 cell lines (Table 3 and Figure 4). All of the five cell lines showing dense promoter methylation were shown to be negative for maspin expression using real-time PCR. Conversely, all of the cell lines without detectable transcripts demonstrated promoter methylation, except for two cell lines, ACC-LC-172 (SCLC) and VMRC-LCD (adenocarcinoma).

In the normal tissues, no expression was observed in the peripheral lung and, consistently, the promoter region of the maspin gene in the tissues was densely methylated. Methylation of the six peripheral lung tissues reached 89.6% on average. Similarly, 91.5% of CpG sites examined were methylated in lymph nodes, where no maspin expression was detected. In contrast, percentage methylation of microdissected bronchial

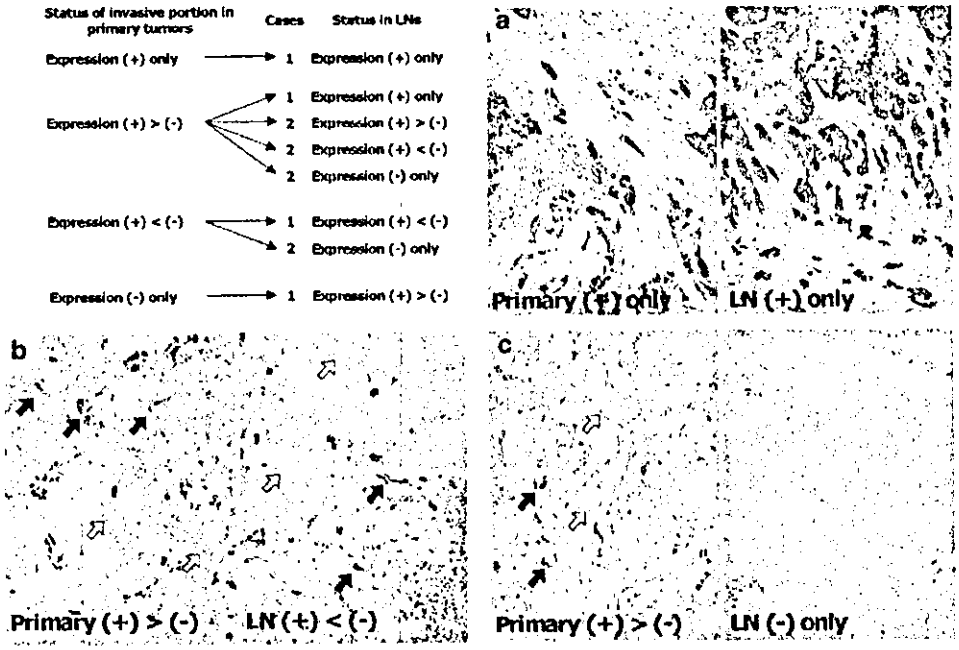

Figure 3 Summarized results of the comparison of expression status between primary and metastatic sites in cases with heterogeneous expression and lymph node metastasis. Half of the tumors showed an identical or increased expression pattern between primary and metastatic sites, whereas decreased expression in metastatic sites was observed in the other half. Three representative pictures (a–c) of maspin expression in primary tumors (left, labeled as primary) and the corresponding lymph nodes (right, labeled as LN) are displayed. Arrows indicate maspin-positive (closed) and -negative (open) tumor cells

Table 3 Summary of methylation status with bisulfite genomic sequencing

	N	*Expression*	*% Methylation*
Cell lines[a]		*Maspin mRNA/18 s rRNA*	
Small cell carcinoma	3	0/2/0[b]	0/0/100[c]
Adenocarcinoma	4	232/29/17/1	0/0/0/0
Adenocarcinoma	2	0/0	95/0
Squamous cell carcinoma	3	0/0/11	90/98/0
Large cell carcinoma	1	0	58
Normal tissues		*IHC results*	
Peripheral lung	6	Almost negative	85/88/88/90/92/95
Bronchial epithelium	2	Positive in basal cells	32/43
Lymph node	2	Completely negative	91/92
Tumors		*IHC results*	
Squamous cell carcinoma	6	Mostly positive	1/1/1/2/3/4
Adenocarcinoma	6	Mostly positive	0/0/1/7/23/18
Adenocarcinoma	7	Mostly negative	0/34/35/46/65/91/98
Adenocarcinoma	3	Positive portion	23/1/37[d]
		Negative portion	46/39/71

[a]Cell lines used include ACC-LC172, ACC-LC80, SK-LC2 for SCLC, SK-Lu-1, ACC-LC319, RERF-LC-MT, SK-LC3 for AD-mRNA positive, ACC-LC94, VMRC-LCD for AD-mRNA negative, RERF-LC-AI, SK-MES1, QG56 for squamous cell carcinoma, and Calu6 for large cell carcinoma. [b]In order corresponding to that listed in footnote a. [c]In order corresponding to that in column expression. [d]Positive and negative portions are separately displayed from case 1–3

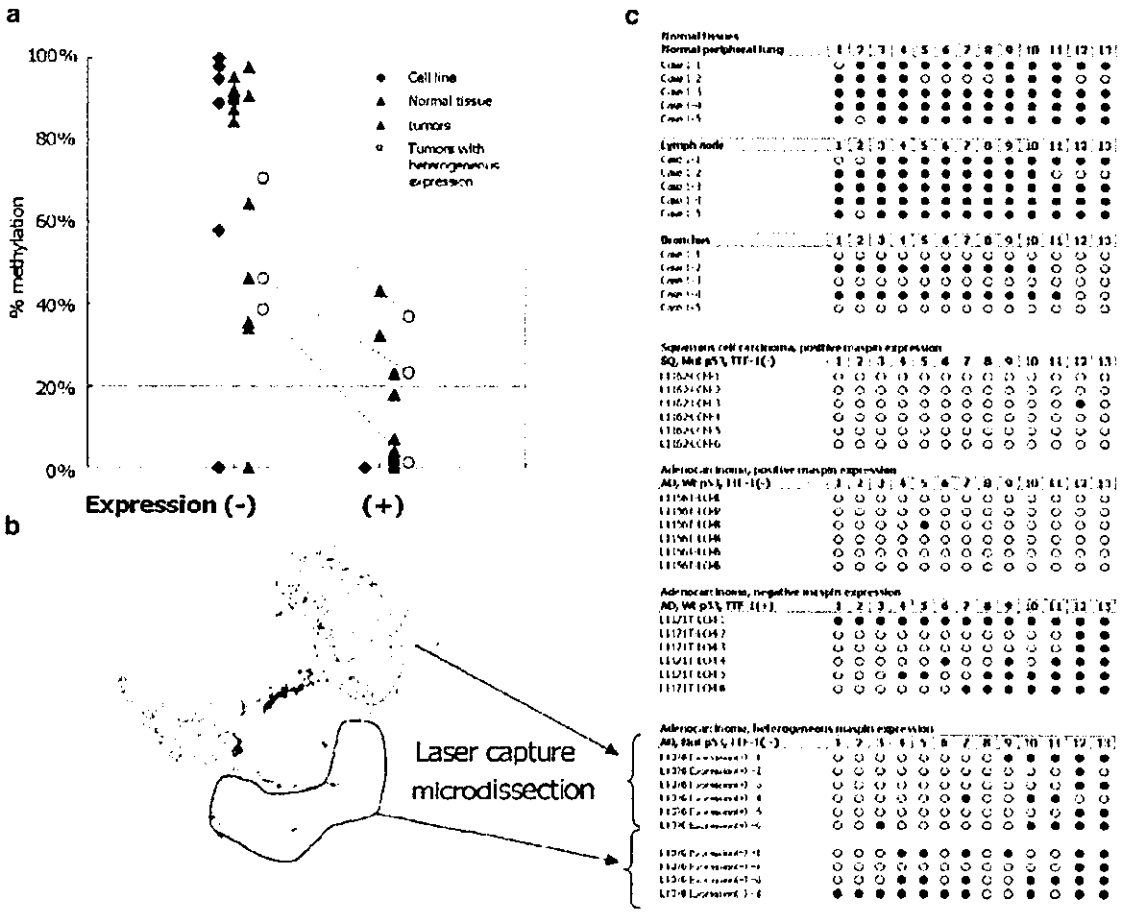

Figure 4 Relationship between promoter DNA methylation and expression status in normal lung tissue, lung cancer cell lines and non-small-cell carcinoma *in vivo* (a). Lines in the chart between positive and negative expression indicate the shift in methylation patterns between positive and negative portions in individual cases with heterogeneous expression, which were examined separately. A representative frozen section examined is shown (b). Positive and negative portions were separately microdissected and examined. Representative results are listed in (c)

epithelium from two individuals was 32.3 and 43.1%. Bronchial epithelium was only a part of the lung tissue that expressed maspin, but the expression was limited to the basal layer. The whole layer of bronchial epithelium was able to be microdissected, and thus, the results represented the methylation status of mixed bronchial epithelium with and without maspin expression. These results indicated that methylation and expression are well correlated, suggesting cell-type-associated promoter DNA methylation.

We then examined the correlation of expression and methylation status in tumors *in vivo* (Table 3). As in normal tissue, six of the squamous cell carcinoma and six adenocarcinomas with uniform maspin expression had almost no methylated CpG sites in the promoter region of maspin gene (2.0 and 8.2% on average, respectively). Methylation patterns in seven adenocarcinomas without maspin expression were contrasted, and the promoter region was methylated in six of the seven tumors. In three adenocarcinomas with heterogeneous expression, portions with and without maspin expression were separately microdissected, and the methylation status was independently accessed. The portions without detectable maspin expression contained a more intensely methylated promoter than that with maspin expression (Figure 4). The results suggested that the expression of maspin was correlated with methylation status both between and within tumors.

Discussion

The current study demonstrated that maspin is not expressed in the lung parenchyma, but specifically in bronchial epithelium, of which basal cells were the predominant source of expression. As promoter DNA methylation in the bronchial epithelium was contrasted to that in lung parenchyma, this suggests that the expression is associated with promoter DNA methylation. This observation extends the finding of Futscher *et al.* (2002) that promoter hypermethylation plays a role in the maintenance of cell-specific expression. Differences in whole genomic methylation patterns among various tissues with restriction landmark genomic scanning (Kawai *et al.*, 1993) also supports the hypothesis.

It has been widely accepted that promoter DNA hypermethylation is one of the mechanisms that inactivate tumor suppressor gene. Although maspin is frequently documented to function as a tumor suppressor *in vitro*, current work suggests that the expression status of maspin in non-small-cell lung cancers is reflected in its expression in corresponding normal lung tissues. Selective expression of maspin in normal proximal airway cells suggests that maspin may be expressed in association with proximal airway cell type. Indeed, uniform expression of maspin in squamous cell carcinoma is consistent with the idea that squamous cell carcinoma is likely to be derived from proximal airway cells through the metaplasia–dysplasia–carcinoma sequence. We have recently reported that TTF-1 is useful for the distinction of peripheral airway cell-derived adenocarcinomas (Yatabe *et al.*, 2002). The expression status of TTF-1 is inversely correlated with that of maspin in adenocarcinomas, suggesting that maspin expression is not associated with the role of tumor suppressor, but that simply is a reflection of the cell type of the proximal airway cells. This may explain the discrepancies between several reports examining tumors *in vivo* and suggesting a role *in vitro*. For example, in breast cancers, two articles have reported that maspin expression is associated with a higher histological grade, lack of estrogen receptor expression and poor prognosis (Umekita *et al.*, 2002; Bieche *et al.*, 2003). Nevertheless, breast cancer cell lines, which were transfected with the maspin gene, suppressed motility and invasion *in vitro* (Zou *et al.*, 1994; Sheng *et al.*, 1996). Linkage of the discrepant findings may be present in the fact that maspin expression is restricted to the basal/myoepithelium of the ducts in the normal breast. According to the molecular profiles, cDNA microarray analysis subdivides breast cancers into three subtypes, which include luminal, basal and ERBB2$^+$ types (Perou *et al.*, 2000; Sorlie *et al.*, 2003). One of the subtypes, the basal cell type, is characterized by (1) high expression of the basal cell markers, cytokeratin 5 and 17; (2) negative expression of estrogen receptor and progesterone; and (3) clinical aggressiveness. Although the expression status of maspin is not available in the classification, the characteristics of this basal cell type resembles those of maspin-expressing tumors, suggesting that maspin expression in breast cancers may also be simply reflected in certain cellular properties rather than tumor-suppressive function of maspin. This hypothesis does not deny the finding observed *in vitro* and, indeed, maspin expression was decreased in metastatic cancer cells in the lymph nodes, as shown in this study.

Another point of interest is that intratumor heterogeneity is partly mediated by promoter DNA methylation. We have previously reported that the allelic loss of 2q, 9p and 22q, which are associated with the advanced stage of tumors, varied in individual tumors, and that the diversity is related to morphological tumor grade (Yatabe *et al.*, 2000). The present study revealed that gene silencing by DNA methylation is another contributor to intratumor heterogeneity. In general, DNA methylation is stable and inheritable over cell divisions. However, selective pressure during the tumor progression may alter the pattern. Indeed, a reversible shift in methylation pattern between monolayer and spheroid culture has been reported (Graff *et al.*, 2000). A recent article by Kang *et al.* (2003) proposed the hypothesis that metastasis is enhanced by intratumor clonal diversity superimposed on a background of poor-prognosis signature property.

Infiltrating cancer cells to the stroma in small clusters are conceivable as a source of metastasis. In the current study, when the expression status is compared between the clusters and metastatic cancer cells, decreased expression is observed in half of the cases with heterogeneous expression and lymph node metastasis.

This is compatible with the results *in vitro* that maspin functions as an invasion suppressor. However, in another comparison with a low-grade lesion and the infiltrating portion of individual tumors, the infiltrating portion expressed maspin. These findings appear to be in conflict. A similar complex issue was addressed by Graff *et al.* (2000). E-cadherin is known to be heterogeneously expressed throughout all stages of malignant progression, including primary and metastatic tumors. They revealed a drift in methylation pattern of E-cadherin between monolayer and spheroid culture *in vitro*, suggesting a dynamic, reversible process of methylation in tumors. Based on the results, they speculated that a portion of tumor cells with decreased E-cadherin expression preferentially infiltrate to the stroma and metastasize to the lymph nodes. This is followed by an expansion of the E-cadherin-expressing portion in lymph nodes to survive in the microenvironment, because restoration of E-cadherin facilitates proliferation and cell survival through cell-to-cell interaction (Day *et al.*, 1999). Thus, the status in lymph nodes appears heterogeneous. Maspin may follow a similarly complex scenario. Alternatively, different processes may be involved between heterogeneous maspin expression in tumors and decreased expression in lymph nodes. Preferential expression of maspin in high histological grade tumors and in solid/infiltrating portions in individual tumors suggests the following hypothesis. Generally, maspin is expressed in accordance with the cell type. As tumors progress, the methylation maintenance system is impaired, and it alters some expression, including maspin, that results in increased heterogeneity in the individual tumors. Then, metastatic clone(s) is selected among the heterogeneous cell population according to its metastatic potential, and metastasizes to lymph nodes. This explains the findings obtained, and lack of expression in preneoplastic and *in situ* lesions of the peripheral type of adenocarcinoma supports the hypothesis.

Maspin is one of the target genes of the p53 pathway. It has been shown that mutated p53 lacks an ability to induce maspin (Zou *et al.*, 2000), and that restoration of wild-type p53 and inhibition of DNA methylation by 5-aza-doxycytidine treatment reactivate maspin expression (Oshiro *et al.*, 2003). In the current study, correlation between maspin expression and p53 status in lung cancers was not clear, and the expression status of maspin was not affected by p53 status in cases without promoter methylation. This implies that cell-type-specific expression of maspin might function differently from induced maspin that is mediated by p53. However, two cell lines and a case of adenocarcinoma, showing a negative expression of maspin (despite no promoter hypermethylation), exhibited mutated p53. p53 may modulate the expression in some occasions. In contrast, K-*ras* status was associated with maspin expression in lung adenocarcinoma. It has been reported that mucinous bronchioloalveolar carcinoma (BAC) preferentially harbors a K-*ras* mutation (Tsuchiya *et al.*, 1995; Marchetti *et al.*, 1996). Mucinous BAC is composed of neoplastic cells resembling goblet cells, which are present in the proximal airway tracts in the normal tissue. Although the mucinous BAC spreads over the peripheral lungs in a manner similar to lepidic growth, a marker of peripheral airway cells, TTF-1, is mostly negative (Goldstein and Thomas, 2001; Lau *et al.*, 2002), suggesting proximal airway-associated tumors of mucinous BAC. Therefore, prevalence of K-*ras* mutations in maspin-positive adenocarcinoma might represent maspin expression in association with cell type of proximal airway cells.

It is of no doubt that the accumulation of genetic and epigenetic alterations generates a tumor. The alterations are not always the same among a certain group of tumors. Indeed, a metastatic tumor is categorized as being adjacent to the primary tumor among any other tumors with unsupervised hierarchical clustering of expression profiles. The current study used a cross-sectional analysis to illustrate the difference in methylation patterns in individual tumors. The analysis gives the ability to reveal real differences independent of the background of the alterations. The analysis can be applied to various methods, including chromatin immunoprecipitation and expression profile analysis, and the results may shed light on complex phenomena in tumors *in vivo*.

Materials and methods

Patients

A series of 145 consecutive, non-small-cell carcinoma cases presenting between September 2000 and December 2002 at the Department of Pathology and Molecular Diagnostics, Aichi Cancer Center, Nagoya, Japan were used for the present study. In addition, five cases of atypical adenomatous hyperplasia and five cases of nonmucinous BAC were examined to determine the expression status in premalignant and *in situ* neoplasia. Pathological staging was determined according to the AJCC Cancer Staging Manual (Greene *et al.*, 2002).

Tissue microarray

In order to represent a whole tissue, four regions were selected per tumor, and tissue microarrays were constructed with an MTA-1 manual tissue arrayer (Beecher Instruments, Inc., Silver Spring, MD, USA). Briefly, selected regions of the donor paraffin block were punched with a 0.6 mm core needle, transferred and arrayed in the recipient block using the arrayer. Serial 4 μm thick sections were then placed on coated glass slides for immunohistochemical analysis.

Immunohistochemistry

Immunohistochemical examination was performed with the standard avidin–biotin–peroxidase complex method using the monoclonal antibodies against maspin (G167-70, BD Bioscience Pharmingen, San Diego, CA, USA), TTF-1 (8G7G3, DAKO, Copenhagen Denmark) and surfactant precursor protein B (19H7, Novocastra, Newcastle upon Tyne, UK). Antigens were retrieved by autoclave. Some of the tissue cores, which were missing during the procedure, or unable to be evaluated, were excluded from the analysis. Each core stained was evaluated semiquantitatively for the following criteria. A greater than moderate intensity of signal was

considered as positive, and the proportion was scored as 0 = negative, 1 = less than 50% positive tumor cells and 2 = equal to or more than 50% positive tumor cells. Averaged scores were calculated, and each case was categorized into 'mostly positive' when the averaged score was more than or equal to 1.75, 'mostly negative' when less than or equal to 0.25 and 'heterogeneous' when the score was greater than 0.25 and less than 1.75. The expression status in all cases in the heterogeneous category and 15 cases each of the mostly positive and mostly negative category was verified with staining of the corresponding whole sections.

Relative quantification by real-time RT–PCR

Total RNA was extracted from 13 cell lines, and first-strand cDNAs were synthesized using Superscript II (Invitrogen, Carlsbad, CA, USA) and random hexamer primers (Roche Applied Science, Alameda, CA, USA). Real-time quantitative PCR amplifications were performed with the Smart Cycler system (SC-100, Cepheid, Sunnyvale, CA, USA). The reactions were carried out using the QuantiTect SYBR Green PCR kit (Qiagen, Valencia, CA, USA). In each reaction, standard samples were diluted up to 1/1000 with cDNA from a lung cancer cell line, selected in preliminary experiments for each gene, and were run with unknown tumor samples. Finally, relative quantitative values from each sample were compared to their 18s rRNA values.

*Mutation status of p53 and K-*ras

Frozen tissue of the tumor specimens was grossly dissected to enrich for the tumor cells and to extract total RNA with the RNeasy kit (Qiagen). Using a standard RT–PCR procedure, exon 4 to exon 10 of the p53 gene was amplified, and the products directly sequenced with an ABI PRISM 310 Genetic Analyzer (Applied Biosystems, Foster City, CA, USA). When no mutation signals were obtained, the result was confirmed by a functional assay in yeast (Ishioka *et al.*, 1993; Waridel *et al.*, 1997). When more than 10% of red colonies or significant deviation of the split assay using pWF35 and pFW34 were observed with the functional assay, RNA was re-extracted from tumor cells removed with a laser-captured microdissection system (PixCell-II, Arcturus, CA, USA), and the products of RT–PCR were sequenced. Using the same RNA as the p53 mutational analysis, the K-*ras* mutation was examined with direct sequencing.

Analysis of methylation status

Methylation status of the maspin promoter was examined in representative cases, including eight cases with uniformly positive expression, five cases with completely negative expression and three cases with heterogeneous expression, where the positive and negative portions were analysed separately. Genomic DNA was microdissected from frozen tissues mounted in OCT compound, to ensure that over 90% of the extract was derived from tumor cells, using a laser captured microdissection system. Then, bisulfite genomic sequencing was performed as previously described (Yatabe *et al.*, 2001). Briefly, converted DNA was amplified with maspin-specific primers based on the sequence obtained from Genebank (Accession NT_033907). The PCR product contained 13 CpG sites, was 153 bp downstream from an *Msp*I site (Zou *et al.*, 1994; Futscher *et al.*, 2002), and the product was located between the p53 binding site 1 and 2 (Zou *et al.*, 2000). The primer sequences were: forward, 5′-TGTTAA-GAGGTTTGAGTAGGAGAGG-3′ and reverse, 5′-CCCACCTTACTTACCTAAAATCACAAT-3′. Amplified products were cloned (TOPO TA cloning kit, Invitrogen, Carlsbad, CA, USA), and five or more clones per case were sequenced. The averaged percentage of CpG sites was considered for methylation status of the case or tumor portion.

Statistical analysis

The χ^2 test for independence and unpaired *t*-test compared incidences of maspin expression and frequencies of clinicopathologic variables. A *P*-value below 0.05 was considered statistically significant.

Acknowledgements
We thank Richard D Iggo for the kind gift of the FASAY plasmids and yeast strains, Kaori Hayashi for excellent technical assistance with the molecular genetic experiments and Hiroji Ishida for assistance in constructing the tissue array. This study is supported by Grant-in-Aid for Encouragement of Young Scientists (B) from the Ministry of Education, Science, Sports and Culture, Japan.

References

Achiwa H, Yatabe Y, Hida T, Kuroishi T, Kozaki K, Nakamura S, Ogawa M, Sugiura T, Mitsudomi T and Takahashi T. (1999). *Clin. Cancer Res.*, **5**, 1001–1005.

Bass R, Fernandez AM and Ellis V. (2002). *J. Biol. Chem.*, **277**, 46845–46848.

Bhattacharjee A, Richards WG, Staunton J, Li C, Monti S, Vasa P, Ladd C, Beheshti J, Bueno R, Gillette M, Loda M, Weber G, Mark EJ, Lander ES, Wong W, Johnson BE, Golub TR, Sugarbaker DJ and Meyerson M. (2001). *Proc. Natl. Acad. Sci. USA*, **98**, 13790–13795.

Bieche I, Girault I, Sabourin JC, Tozlu S, Driouch K, Vidaud M and Lidereau R. (2003). *Br. J. Cancer*, **88**, 863–870.

Day ML, Zhao X, Vallorosi CJ, Putzi M, Powell CT, Lin C and Day KC. (1999). *J. Biol. Chem.*, **274**, 9656–9664.

Domann FE, Rice JC, Hendrix MJ and Futscher BW. (2000). *Int. J. Cancer*, **85**, 805–810.

Futscher BW, Oshiro MM, Wozniak RJ, Holtan N, Hanigan CL, Duan H and Domann FE. (2002). *Nat. Genet.*, **31**, 175–179.

Garber ME, Troyanskaya OG, Schluens K, Petersen S, Thaesler Z, Pacyna-Gengelbach M, van de Rijn M, Rosen GD, Perou CM, Whyte RI, Altman RB, Brown PO, Botstein D and Petersen I. (2001). *Proc. Natl. Acad. Sci. USA*, **98**, 13784–13789.

Goldstein NS and Thomas M. (2001). *Am. J. Clin. Pathol.*, **116**, 319–325.

Graff JR, Gabrielson E, Fujii H, Baylin SB and Herman JG. (2000). *J. Biol. Chem.*, **275**, 2727–2732.

Greene FL, Page DL, Fleming ID, Fritz AG, Balch CM, Haller DG and Morrow M (eds) (2002). *AJCC Cancer Staging Manual*, 6th edn. Springer-Verlag: New York.

Ishioka C, Frebourg T, Yan YX, Vidal M, Friend SH, Schmidt S and Iggo R. (1993). *Nat. Genet.*, **5**, 124–129.

Jiang N, Meng Y, Zhang S, Mensah-Osman E and Sheng S. (2002). *Oncogene*, **21**, 4089–4098.

Jones PA and Baylin SB. (2002). *Nat. Rev. Genet.*, **3**, 415–428.

Kang Y, Siegel PM, Shu W, Drobnjak M, Kakonen SM, Cordon-Cardo C, Guise TA and Massague J. (2003). *Cancer Cell*, **3**, 537–549.

Kawai J, Hirotsune S, Hirose K, Fushiki S, Watanabe S and Hayashizaki Y. (1993). *Nucleic Acids Res.*, **21**, 5604–5608.
Laird PW. (2003). *Nat. Rev. Cancer*, **3**, 253–266.
Lau SK, Desrochers MJ and Luthringer DJ. (2002). *Mod. Pathol.*, **15**, 538–542.
Li E, Beard C and Jaenisch R. (1993). *Nature*, **366**, 362–365.
Maass N, Biallek M, Rosel F, Schem C, Ohike N, Zhang M, Jonat W and Nagasaki K. (2002). *Biochem. Biophys. Res. Commun.*, **297**, 125–128.
Maass N, Hojo T, Ueding M, Luttges J, Kloppel G, Jonat W and Nagasaki K. (2001). *Clin. Cancer Res.*, **7**, 812–817.
Marchetti A, Buttitta F, Pellegrini S, Chella A, Bertacca G, Filardo A, Tognoni V, Ferreli F, Signorini E, Angeletti CA and Bevilacqua G. (1996). *J. Pathol.*, **179**, 254–259.
Markl ID, Cheng J, Liang G, Shibata D, Laird PW and Jones PA. (2001). *Cancer Res.*, **61**, 5875–5884.
Mohandas T, Sparkes RS and Shapiro LJ. (1981). *Science*, **211**, 393–396.
Nass SJ, Herman JG, Gabrielson E, Iversen PW, Parl FF, Davidson NE and Graff JR. (2000). *Cancer Res.*, **60**, 4346–4348.
Nishio M, Koshikawa T, Yatabe Y, Kuroishi T, Suyama M, Nagatake M, Sugiura T, Ariyoshi Y, Mitsudomi T and Takahashi T. (1997). *Clin. Cancer Res.*, **3**, 1051–1058.
Oshiro MM, Watts GS, Wozniak RJ, Junk DJ, Munoz-Rodriguez JL, Domann FE and Futscher BW. (2003). *Oncogene*, **22**, 3624–3634.
Perou CM, Sorlie T, Eisen MB, van de Rijn M, Jeffrey SS, Rees CA, Pollack JR, Ross DT, Johnsen H, Akslen LA, Fluge O, Pergamenschikov A, Williams C, Zhu SX, Lonning PE, Borresen-Dale AL, Brown PO and Botstein D. (2000). *Nature*, **406**, 747–752.
Sheng S, Carey J, Seftor EA, Dias L, Hendrix MJ and Sager R. (1996). *Proc. Natl. Acad. Sci. USA*, **93**, 11669–11674.
Sheng S, Pemberton PA and Sager R. (1994). *J. Biol. Chem.*, **269**, 30988–30993.
Sood AK, Fletcher MS, Gruman LM, Coffin JE, Jabbari S, Khalkhali-Ellis Z, Arbour N, Seftor EA and Hendrix MJ. (2002). *Clin. Cancer Res.*, **8**, 2924–2932.
Sorlie T, Tibshirani R, Parker J, Hastie T, Marron JS, Nobel A, Deng S, Johnsen H, Pesich R, Geisler S, Demeter J, Perou CM, Lonning PE, Brown PO, Borresen-Dale AL and Botstein D. (2003). *Proc. Natl. Acad. Sci. USA*, **100**, 8418–8423.
Tsuchiya E, Furuta R, Wada N, Nakagawa K, Ishikawa Y, Kawabuchi B, Nakamura Y and Sugano H. (1995). *J. Cancer Res. Clin. Oncol.*, **121**, 577–581.
Umekita Y, Ohi Y, Sagara Y and Yoshida H. (2002). *Int. J. Cancer*, **100**, 452–455.
Waridel F, Estreicher A, Bron L, Flaman JM, Fontolliet C, Monnier P, Frebourg T and Iggo R. (1997). *Oncogene*, **14**, 163–169.
Yatabe Y, Hida T, Achiwa H, Muramatsu H, Kozaki K, Nakamura S, Ogawa M, Mitsudomi T, Sugiura T and Takahashi T. (1998a). *Cancer Res.*, **58**, 3761–3764.
Yatabe Y, Konishi H, Mitsudomi T, Nakamura S and Takahashi T. (2000). *Am. J. Pathol.*, **157**, 985–993.
Yatabe Y, Masuda A, Koshikawa T, Nakamura S, Kuroishi T, Osada H, Takahashi T, Mitsudomi T and Takahashi T. (1998b). *Cancer Res.*, **58**, 1042–1047.
Yatabe Y, Mitsudomi T and Takahashi T. (2002). *Am. J. Surg. Pathol.*, **26**, 767–773.
Yatabe Y, Tavare S and Shibata D. (2001). *Proc. Natl. Acad. Sci. USA*, **98**, 10839–10844.
Zhang M, Volpert O, Shi YH and Bouck N. (2000). *Nat. Med.*, **6**, 196–199.
Zou Z, Anisowicz A, Hendrix MJ, Thor A, Neveu M, Sheng S, Rafidi K, Seftor E and Sager R. (1994). *Science*, **263**, 526–529.
Zou Z, Gao C, Nagaich AK, Connell T, Saito S, Moul JW, Seth P, Appella E and Srivastava S. (2000). *J. Biol. Chem.*, **275**, 6051–6054.

Oncogene (2004), 1–11

www.nature.com/onc

ORIGINAL PAPER

Gene expression-based, individualized outcome prediction for surgically treated lung cancer patients

Shuta Tomida[1,6], Katsumi Koshikawa[1,6], Yasushi Yatabe[2], Tomoko Harano[1], Nobuhiko Ogura[3], Tetsuya Mitsudomi[4], Masato Some[3], Kiyoshi Yanagisawa[1], Toshitada Takahashi[5], Hirotaka Osada[1] and Takashi Takahashi*[,1]

[1]*Division of Molecular Oncology, Aichi Cancer Center Research Institute, Nagoya 464-8681, Japan;* [2]*Department of Pathology and Molecular Diagnostics, Aichi Cancer Center Hospital, Nagoya 464-8681, Japan;* [3]*Miyanodai Technology Development Center, Fuji Photo Film Co., Ltd., Kanagawa 258-8538, Japan;* [4]*Department of Thoracic Surgery, Aichi Cancer Center Hospital, Nagoya 464-8681, Japan;* [5]*Division of Immunology, Aichi Cancer Center Research Institute, Nagoya 464-8681, Japan*

Individualized outcome prediction classifiers were successfully constructed through expression profiling of a total of 8644 genes in 50 non-small-cell lung cancer (NSCLC) cases, which had been consecutively operated on within a defined short period of time and followed up for more than 5 years. The resultant classifier of NSCLCs yielded 82% accuracy for forecasting survival or death 5 years after surgery of a given patient. In addition, since two major histologic classes may differ in terms of outcome-related expression signatures, histologic-type-specific outcome classifiers were also constructed. The resultant highly predictive classifiers, designed specifically for nonsquamous cell carcinomas, showed a prediction accuracy of more than 90% independent of disease stage. In addition to the presence of heterogeneities in adenocarcinomas, our unsupervised hierarchical clustering analysis revealed for the first time the existence of clinicopathologically relevant subclasses of squamous cell carcinomas with marked differences in their invasive growth and prognosis. This finding clearly suggests that NSCLCs comprise distinct subclasses with considerable heterogeneities even within one histologic type. Overall, these findings should advance not only our understanding of the biology of lung cancer but also our ability to individualize postoperative therapies based on the predicted outcome.
Oncogene advance online publication, 5 April 2004; doi:10.1038/sj.onc.1207697

Keywords: lung cancer; gene expression profile; microarray; prognosis

Introduction

Lung cancer is the most prevalent and deadly cancer in economically developed countries. In the US, more than 170 000 people die annually due to lung cancer, while Japan is facing a continuing and steep increase in lung cancer deaths with loss of more than 51 000 lives annually. Lung cancers are classified into two major groups, small-cell lung cancer and non-small-cell lung cancer (NSCLC), based on their clinicopathologic characteristics. Owing to the considerable differences in their etiologies, genetic and epigenetic changes and clinicopathologic features, NSCLCs are often further subgrouped into two major categories, that is, squamous cell carcinomas and nonsquamous cell carcinomas (Minna *et al.*, 1997; Osada and Takahashi, 2002).

Surgical resection gives the best hope for a cure for NSCLC cases, which comprise 80–85% of lung cancers. Unfortunately, however, their long-term survival rate remains unsatisfactory and no more than 50% of the cases that have successfully undergone potentially curative resection can survive for 5 years after operation. The TNM classification according to tumor size, extent of nodal involvement and the presence or absence of distant metastasis is routinely used as a prognostic tool, but it only provides information about what percentage of cases at a particular disease stage, which a given patient belongs to, can be expected to be alive at specific postoperative time points. Although various genetic and epigenetic changes of cancer-related genes have been identified and examined in the search for clinically relevant prognosticators, no single variable thus far evaluated has proven to be sufficiently predictive to accurately forecast a patient's outcome (Slebos *et al.*, 1990; Horio *et al.*, 1993; Mitsudomi *et al.*, 2000).

Recent rapid progress in microarray technology has made it possible to analyse gene expression profiles on a genome-wide basis in order to search for molecular markers for cancer classification and outcome prediction (Golub *et al.*, 1999; Alizadeh *et al.*, 2000; Perou *et al.*, 2000; Khan *et al.*, 2001; Pomeroy *et al.*, 2002; Ye *et al.*, 2003). While lung cancers are known to be very

*Correspondence: T Takahashi, Division of Molecular Oncology, Aichi Cancer Center Research Institute, 1-1 Kanokoden, Chikusa-ku, Nagoya 464-8681, Japan:
E-mail: tak@aichi-cc.jp
[6]ST and KK contributed equally to this work
Received 5 January 2004; revised 23 February 2004; accepted 1 March 2004

heterogeneous in various aspects as clearly mentioned, recent expression profiling studies have shown the presence of several subclasses with distinct expression profiles not only among NSCLC but also and specifically among adenocarcinoma (Bhattacharjee *et al.*, 2001; Garber *et al.*, 2001; Beer *et al.*, 2002; Virtanen *et al.*, 2002). However, the existence of clinically relevant subclasses of squamous cell carcinomas in terms of expression profiles has not been detected thus far, while development of an individualized outcome classifier is eagerly awaited in the hope of implementing tailor-made treatments for this fatal disease.

In the study presented here, a consecutively operated, well-defined cohort of 50 NSCLC cases, followed up for more than 5 years, was used to acquire expression profiles of a total of 8644 unique genes, leading to the successful construction of supervised learning method-based individualized outcome prediction classifiers with high accuracy. In addition, the identification by means of unsupervised hierarchical clustering analysis of two distinct subclasses of squamous cell carcinomas with interesting histologic distinctions and a significant difference in their prognosis is also reported.

Results

Unsupervised hierarchical clustering of NSCLCs

We first applied unsupervised hierarchical clustering algorithm to a comparison of gene expression profiles of 50 NSCLC cases using the filtered 900 spots corresponding to 829 unique genes that had passed our filtering procedures. The resulting clusters recapitulated the distinctions between well-established histologic classes of NSCLCs, that is, squamous cell and nonsquamous cell carcinomas (Figures 1a–f), and the results of immunohistochemical analysis of TTF-1 and cytokeratin 7 (KRT7) expression, which used tissue microarrays containing all of the cases examined in this study, were consistent with those of the cDNA microarray analysis (data not shown). We noted that squamous cell carcinomas formed a more discrete cluster than nonsquamous cell carcinomas, demonstrating the generally strong expression of several well-accepted differentiation markers of squamous epithelium including cytokeratins 5 and 13, S100A2 and galectin 7 (LGALS7) (Figure 1d) (Magnaldo *et al.*, 1998; Chu and Weiss, 2002). Markedly high-level expression of small proline-rich proteins such as SPRR1B and SPRR2C was also generally observed in squamous cell carcinomas (Hu *et al.*, 1998). While squamous cell carcinomas were clustered as a large single cluster, there appeared to be two major subclasses of squamous cell carcinomas in relation to the gene expression profiles, and the distinctions between the two subclasses could be even more clearly illustrated in the separate hierarchical clustering analysis of squamous cell carcinomas (data not shown). Squamous cell carcinoma cluster 1 (SQ1) expressed a characteristic set of genes that are related to extracellular matrix proteins, including fibronectin and various collagen subunits such as α2(I) and α1(III) (Figure 1f), as well as those related to DNA replication and cell proliferation including ARAF1 and EPHA1 (Figure 1e) (Shelton *et al.*, 2003; Walker-Daniels *et al.*, 2003). Interestingly, patients belonging to the SQ1 cluster had a significantly poorer prognosis after potentially curative resection than those of SQ2 (Figure 2a, $P=0.013$ by log-rank test). Another prominent distinction between SQ1 and SQ2 was their growth patterns. Seven of the eight (88%) cases of SQ1 showed an infiltrative growth pattern with dense fibrous stroma in contrast to lack of these features in six of the seven SQ2 tumors ($P=0.010$ by Fisher's exact test), which showed a rather well-circumscribed, expansive growth pattern with inconspicuous keratinization (Figure 2b).

Adenocarcinomas, a major fraction of nonsquamous cell carcinomas, also appeared to be subclassifiable into two major groups according to their expression profiles: adenocarcinoma cluster 1 (AD1) clustered together with squamous cell carcinomas, and AD2, 3 and 4, which formed another distinct cluster. Of the latter subclass, AD3 most typically showed strong expression of peripheral lung cell markers including TTF-1 (TITF1), SP-C (SFTPC) and SP-A (SERPA2) (Figure 1b) (Yatabe *et al.*, 2002). Patients belonging to the AD3 cluster were predominantly female nonsmokers with a well-differentiated adenocarcinoma. In addition, 80% (eight of 10) of the AD3 cases were female subjects in contrast to 29% (six of 21) in non-AD3 adenocarcinoma clusters ($P=0.018$, Fisher's exact test), while well-differentiated tumors were more frequent in AD3 (60%) cases than other adenocarcinoma clusters (14%) ($P=0.015$ by Fisher's exact test). A total of 70% of the AD3 cases were found to be nonsmokers, and this ratio was considerably higher than that for non-AD3 clusters (38%), which in fact contained significantly more heavy smokers (>20 pack years) than AD3 ($P=0.046$ by Fisher's exact test). In marked contrast, AD1 showed low-level expression of peripheral lung markers such as TTF-1 and SP-C and to some extent shared gene expression profiles with squamous cell carcinomas, although they were still clearly distinct. Tumors corresponding to AD2 characteristically showed a strong expression of a number of expressed sequence tags (ESTs), whereas expression of the same set of ESTs was found to be distinctly reduced in AD4 as well as SQ1, suggesting that characterization of these ESTs may shed light on the biology of these tumor subclasses (Figure 1c).

Construction of a survival prediction model for NSCLCs

In order to develop an individualized outcome prediction classifier, we used a signal-to-noise metric first to select genes that most clearly distinguished prognosis-favorable from fatal patients. The unsupervised hierarchical clustering algorithm using the top 100 spots corresponding to 98 unique genes yielded two major branches representing those with favorable and fatal prognosis (Figure 3a). Of the 21 patients in the left or

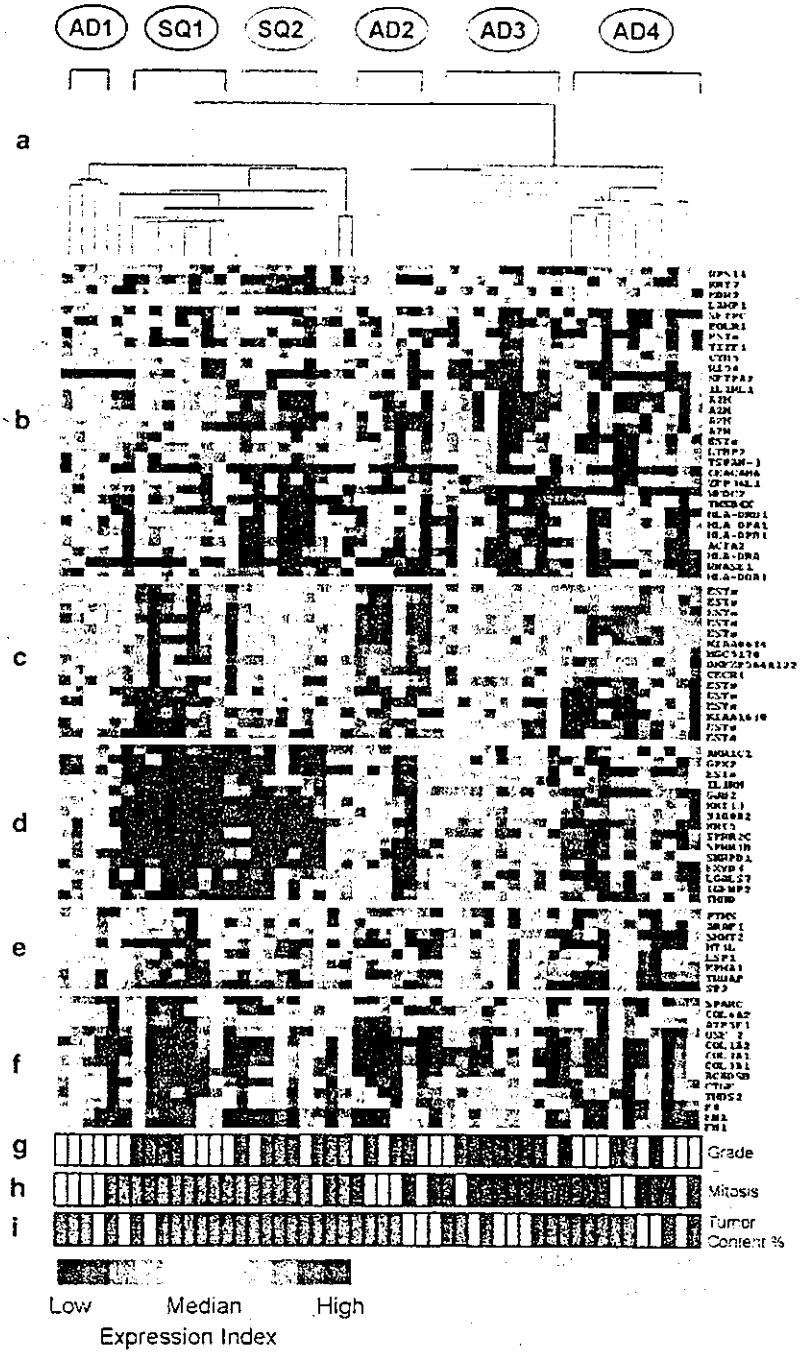

Figure 1 Hierarchical clustering defining subclasses of NSCLCs. (**a**) Dendrogram of two-dimensional hierarchical clustering analysis of the 900 filtered genes across 50 samples of NSCLCs. The expression index for the transcript sequences (rows) in the samples (columns) is indicated by a color code (see expression index in the bar at the bottom of this figure). (**b**) A cluster of genes with high relative expression in adenocarcinomas. (**c**) A gene cluster relevant to AD2. (**d**) A cluster of genes highly expressed in squamous cell lung carcinomas. (**e**, **f**) Cluster of genes with high-level expression in SQ1. (**g**) Histopathologic grade (orange, poor; yellow, moderate; green, well). (**h**) Mitotic indices (green, less than 10 in 10 high-power field; yellow, 10–40; orange, over 40). (**i**) Estimated nucleated tumor content (yellow, 50–74%; orange, more than 75%)

'favorable' branch, 19 had survived 5 years after surgery, while 15 of the 29 cases in the right or 'fatal' branch had died within 5 years after surgery. Their Kaplan–Meier survival curves showed a statistically significant difference (Figure 3b, $P=0.0025$, log-rank test).

Since the ultimate aim was the development of an individualized outcome prediction classifier, we next applied a supervised learning method. To this purpose, a weighted-voting outcome classifier was constructed based on the predictive genes, which were preselected using a signal-to-noise metric. The learning errors for

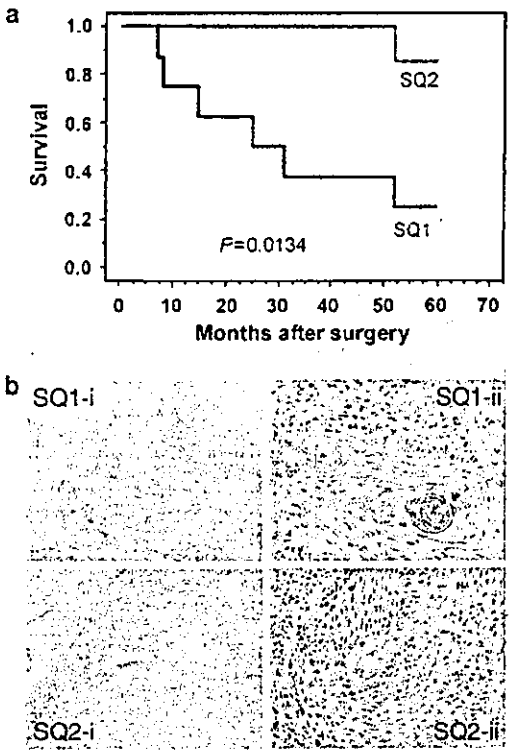

Figure 2 Clinicopathologic distinctions between the SQ1 and SQ2 clusters. (**a**) Kaplan–Meier survival curves of SQ1 and SQ2 showing a significantly different prognosis. (**b**) Representative morphologies of tumors in the SQ1 and SQ2 clusters. Tumors belonging to the SQ1 cluster frequently exhibited invasive growth to surrounding normal lung tissues with active stromal reaction (SQ1-i), while prominent keratinization was a characteristic of SQ1 (SQ1-ii). Tumors of the SQ2 cluster were generally well circumscribed due to their expansive growth (SQ2-i), and minimal stromal reaction is observed in this type. In addition, keratinization and nuclear pleomorphisms were inconspicuous in tumors of SQ2 (SQ2-ii)

Figure 3 Unsupervised hierarchical clustering of 50 NSCLCs according to the expression of top 100 genes by signal-to-noise metric, which distinguish fatal and favorable prognosis. (**a**) Two-dimensional hierarchical with the top 100 predictive genes. (**b**) Kaplan–Meier survival curves for favorable *versus* fatal groups of 50 samples characterized by hierarchical clustering using the top 100 predictive genes

each model, to which increasing numbers of the preselected predictive genes were applied, calculated with the leave-one-out cross-validation method. The weighted-voting model using 25 predictive genes showed the highest accuracy for the prediction of an individual's outcome (Figure 4a), that is, in 41 of 50 (82%) cases. The 25 genes used for constructing the outcome classifier of NSCLCs are listed in Table 1. With this classifier, 27 of 33 (82%) cases, who actually had survived longer than 5 years after surgery, were judged to have a 'favorable' prognosis, while 14 of the 17 (82%) patients who had died within 5 years were correctly predicted as having a 'fatal' outcome (Figure 4b). Survival curves of the patients with 'favorable' and 'fatal' predictions are plotted in Figure 4c, showing a significant difference between the groups ($P = 6.0 \times 10^{-6}$). We also employed other supervised learning algorithms, including the support vector machine and k-nearest neighbors, using increasing numbers of genes as mentioned above. Although accuracies of these models were comparable to that of the weighted-voting outcome classifier, the latter achieved the highest accuracy (data not shown).

Construction of the survival prediction models specific for squamous or nonsquamous cell carcinoma cases

It is generally accepted that squamous cell and nonsquamous cell carcinomas are distinct disease entities in terms of their clinicopathologic features as well as their etiologies (Minna *et al.*, 1997; Osada and Takahashi, 2002). This concept has been supported by the presence of clearly discriminating expression profiles for these two tumor types (Bhattacharjee *et al.*, 2001; Garber *et al.*, 2001; Kikuchi *et al.*, 2003). We therefore constructed outcome prediction classifiers specific for each tumor subtype by using the weighted-voting algorithm and the predictive genes for each subtype selected by signal-to-noise metric. Leave-one-out cross-validation of the classifiers with increasing numbers of

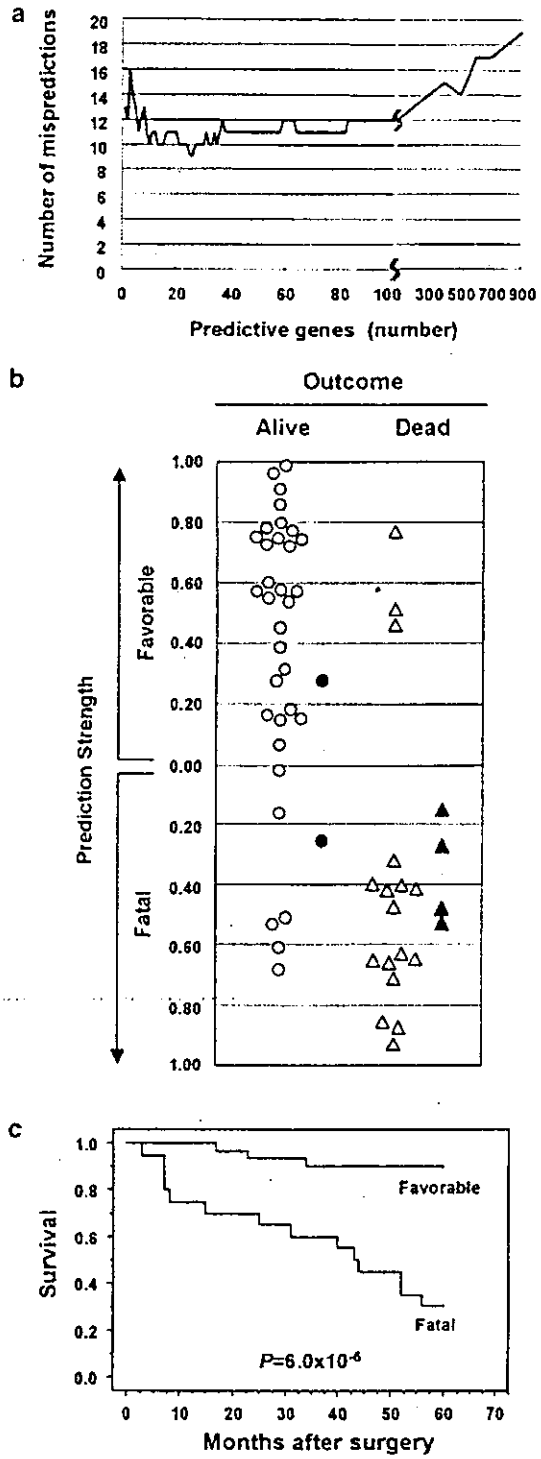

Figure 4 Results of outcome classification by the weighted-voting algorithm using genes preselected with the signal-to-noise metric. (**a**) Search for optimum number of genes for outcome classification. (**b**) Assessment of the outcome classifier using weighted voting algorithm. Open (○) and closed circles (•) indicate patients alive 5 years after surgery, while open (△) and closed triangles (▲) correspond to patients dead within 5 years after surgery. Open marks (○ and △) indicate 50 samples used for leave-one-out cross-validation, while closed marks (• and ▲) indicate additional blinded samples used for independent validation. (**c**) Kaplan–Meier survival curves for the favorable and fatal groups in 50 NSCLC cases predicted by the weighted-voting outcome classifier

the higher-ranked predictive genes yielded the highest accuracies with 12 genes for nonsquamous and 19 genes for squamous cell carcinomas (Tables 2 and 3). Results showed that patients' outcome 5 years after surgery were correctly predicted for 31 of 34 (91%) nonsquamous cell carcinoma cases (Figure 5a). Of the 25 cases judged as having 'favorable' prognosis, 23 (92%) had indeed survived 5 years after surgery, whereas only one of nine (11%) patients predicted as being 'fatal' had survived for 5 years. The differences between survival curves of the 25 patients with the 'favorable' and the nine cases with the 'fatal' prediction were highly significant (Figure 5b, $P=2.4\times10^{-7}$). In the case of squamous cell carcinomas, the weighted-voting model successfully predicted 5-year outcome for 15 of 16 (94%) patients (Figure 5c). Eight of eight (100%) samples judged as being 'favorable' had survived 5 years after surgery, while seven of eight (88%) samples predicted as being 'fatal' had actually died within 5 years. Survival curves based on these predictions showed highly significant differences between the favorable and fatal groups (Figure 5d, $P=3.3\times10^{-5}$).

It was noted that the 12 and 19 genes, which were used to construct the respective outcome classifiers for nonsquamous and squamous cell carcinomas, did not show any overlaps, and histologic-type-specific outcome classifiers contained only two genes each of the top 100, signal-to-noise-preselected genes of the other type of NSCLCs.

Confirmation of the robustness of the classifiers by using an independent blinded validation dataset as well as by random permutation tests

To validate the prognosis classifiers described here, we analysed an additional independent set of six NSCLC cases, three nonsquamous and squamous cell carcinomas each, in a completely blinded fashion. The outcome classifier for both types of NSCLCs correctly predicted the disease outcome in five of the six cases, including the death of a patient with a stage I tumor (Figure 4b). The outcome classifier for nonsquamous cell carcinomas accurately predicted both deaths and one survival (Figure 5a). The outcome classifier for squamous cell carcinomas correctly predicted the outcome for one of the three cases (Figure 5c).

We also performed permutation tests to determine whether the gene sets used in the outcome classifiers were robust, and found highly significant results ($P<0.0001$ in all three classifiers). Through permutation tests analysing 10 000 datasets with permutated class labels, it was shown that outcome classifiers performing with equal or higher accuracy for the initial dataset as well as for the validation dataset could not be obtained by chance association in either NSCLCs ($P=0.0104$) or in nonsquamous cell carcinomas ($P=0.0055$). This type of estimate, however, did not support the statistical significance of the results obtained with squamous cell carcinoma classifier.

Table 1 A total of 25 predictive genes selected for the weighted-voting outcome classifier of NSCLCs

Rank	*Gene*	*Description*	*UniGene ID*	*Class correlation*	P*	*Rank*	
						Non-SQ[a]	*SQ*[a]
1	WEE1	WEE1 homolog	Hs.75188	Fatal	0.0027	2	148
2	MYC	v-myc viral oncogene homolog	Hs.79070	Fatal	0.0057	14	55
3	TITF1	Thyroid transcription factor 1	Hs.197764	Favorable	0.0085	31	65
4	FOSL1	FOS-like antigen 1 (Fra-1)	Hs.283565	Fatal	0.0062	30	135
5	LYPLA1	Lysophospholipase I	Hs.393360	Fatal	0.0081	26	123
6	SSBP1	Single-stranded DNA binding protein	Hs.923	Fatal	0.0199	3	641
7	SFTPC	Surfactant, pulmonary-associated protein C	Hs.1074	Favorable	0.0113	12	290
8	THBD	Thrombomodulin	Hs.2030	Fatal	0.0099	51	14
9	NICE-4	NICE-4 protein	Hs.8127	Fatal	0.0099	1	294
10	PTN	Pleiotrophin (heparin binding growth factor 8)	Hs.44	Fatal	0.0100	38	139
11	SNRPB	Small nuclear ribonucleoprotein polypeptides B and B1	Hs.83753	Fatal	0.0115	10	621
12	NAP1L1	Nucleosome assembly protein 1-like 1	Hs.302649	Fatal	0.0131	46	116
13	CTNND1	Catenin delta 1	Hs.166011	Fatal	0.0120	50	149
14	CCT3	Chaperonin containing TCP1, subunit 3	Hs.1708	Fatal	0.0186	16	515
15	ESTs		Hs.95612	Fatal	0.0160	112	25
16	SPRR1B	Small proline-rich protein 1B (cornifin)	Hs.1076	Fatal	0.0209	70	6
17	COPB	Coatomer protein complex, subunit beta	Hs.3059	Fatal	0.0195	151	17
18	ARG1	Arginase type I (liver)	Hs.332405	Fatal	0.0193	28	435
19	ARCN1	Archain 1 (coatomer protein complex, subunit delta)	Hs.33642	Fatal	0.0169	33	174
20	MST1	Macrophage stimulating 1	Hs.349110	Fatal	0.0193	7	684
21	SERPINE1	Serine (or cysteine) proteinase inhibitor, clade E member 1	Hs.82085	Fatal	0.0194	17	532
22	SERPINB1	Serine (or cysteine) proteinase inhibitor, clade B member 1	Hs.183583	Fatal	0.0205	188	31
23	ESTs		Hs.215113	Favorable	0.0205	36	254
24	ACTR3	Actin-related protein 3 homolog (ARP3)	Hs.380096	Fatal	0.0229	99	67
25	PTP4A3	Protein tyrosine phosphatase type 4A, member 3	Hs.43666	Fatal	0.0199	171	5

*P-values were assigned based upon the frequency, with which signal-to-noise statistics, which were calculated for the 10 000 permutations of the sample labels in each of the nonsquamous cell and squamous cell carcinoma datasets, yielded better results than the actual signal-to-noise statistic. [a]Ranking of the signal-to-noise statistics for the genes in the nonsquamous cell and squamous cell carcinoma datasets

Table 2 A total of 12 predictive genes selected for the weighted-voting outcome classifier of nonsquamous cell carcinomas

Rank	*Gene*	*Description*	*UniGene ID*	*Class correlation*	P*	*Rank in SQ*[a]
1	NICE-4	NICE-4 protein	Hs.8127	Fatal	0.0036	294
2	WEE1	WEE1 homolog	Hs.75188	Fatal	0.0039	148
3	SSBP1	Single-stranded DNA binding protein	Hs.923	Fatal	0.0122	641
4	WFDC2	WAP four-disulfide core domain 2	Hs.2719	Favorable	0.0155	559
5	ACTA2	Actin, alpha 2, smooth muscle, aorta	Hs.195851	Favorable	0.0149	50
6	G22P1	Thyroid autoantigen 70kDa (Ku70)	Hs.197345	Fatal	0.0176	256
7	MST1	Macrophage stimulating 1	Hs.349110	Fatal	0.0153	684
8	PHB	Prohibitin	Hs.75323	Fatal	0.0219	85
9	DRPLA	Dentatorubral-pallidoluysian atrophy	Hs.169488	Fatal	0.0238	749
10	SNRPB	Small nuclear ribonucleoprotein polypeptides B and B1	Hs.83753	Fatal	0.0192	621
11	GJA	Gap junction protein, alpha 1	Hs.74471	Fatal	0.0268	295
12	SFTPC	Surfactant, pulmonary-associated protein C	Hs.1074	Favorable	0.0313	290

*P-values were assigned based upon the frequency, with which signal-to-noise statistics, which were calculated for the 10 000 permutations of the sample labels in the nonsquamous cell carcinoma dataset, yielded better results than the actual signal-to-noise statistic. [a]Ranking of the signal-to-noise statistics for the genes in the squamous cell carcinoma dataset

Discussion

A patient's survival is currently estimated on the basis of empirical information in the TNM classification system about survival distributions according to disease stages. Since survival or death is a matter of all or nothing, currently available information regarding what percentage of those at a certain disease stage are likely to survive after a certain period of time is insufficient in many respects. The study presented here described the successful construction of individualized outcome classifiers as a result of using the gene expression profiling data- and weighted-voting algorithm-based approach, which allowed us to predict outcomes for surgically treated lung cancer patients on an individual basis. Although our outcome classifiers were constructed by using a modestly sized cohort, highly robust prediction models were obtained especially for the prediction of outcome for nonsquamous cell carcinomas, which constitute about 60% of NSCLCs. In fact, patients' 5-year postoperative survival status was correctly predicted for 91% of the leave-one-out cross-validation

Table 3 A total of 12 predictive genes selected for the weighted-voting outcome classifier of squamous cell carcinomas

Rank	*Gene*	*Description*	*UniGene ID*	*Class correlation*	P*	*Rank in non-SQ**
1	ESTs		Hs.28399	Favorable	0.0068	396
2	ESTs		Hs.98269	Favorable	0.0087	178
3	ESTs		Hs.35552	Favorable	0.0034	272
4	KRT5	Keratin 5	Hs.433845	Fatal	0.0046	240
5	PTP4A3	Protein tyrosine phosphatase type 4A, member 3	Hs.43666	Fatal	0.0104	171
6	SPRR1B	Small proline-rich protein 1B	Hs.1076	Fatal	0.0147	70
7	LOC339324	Hypothetical protein LOC339324	Hs.18103	Favorable	0.0171	361
8	MYST4	MYST histone acetyltransferase 4	Hs.27590	Fatal	0.0188	529
9	SPARCL1	SPARC-like 1	Hs.75445	Fatal	0.0210	846
10	IGJ	Immunoglobulin J polypeptide	Hs.76325	Fatal	0.0143	265
11	EIF4A2	Eucaryotic translation initiation factor 4A, isoform 2	Hs.173912	Favorable	0.0233	382
12	ESTs		Hs.261314	Fatal	0.0226	822
13	ID2	Inhibitor of DNA binding 2	Hs.180919	Fatal	0.0214	329
14	THBD	Thrombomodulin	Hs.2030	Fatal	0.0077	51
15	MGC15476	Thymus expressed gene 3-like	Hs.134185	Fatal	0.0231	298
16	ZFP	Zinc-finger protein	Hs.1148	Favorable	0.0217	297
17	COPB	Coatomer protein complex, subunit beta	Hs.3059	Fatal	0.0272	151
18	ZYG	ZYG homolog	Hs.29285	Fatal	0.0237	632
19	CACNA1I	Calcium channel, voltage-dependent, alpha 1I subunit	Hs.125116	Fatal	0.0312	492

**P*-values were assigned based upon the frequency, with which the signal-to-noise statistics, which were calculated for the 10 000 permutations of the sample labels of the squamous cell carcinoma dataset, yielded better results than the actual signal-to-noise statistic. *Ranking of the signal-to-noise statistics for the genes in the nonsquamous cell carcinoma dataset

dataset, and this prediction accuracy was confirmed for the independent validation dataset. It should be noted that the outcome classifier appeared to perform well independently of disease stage; among 24 stage I/II nonsquamous cell carcinoma cases, 17 survivals and five deaths were correctly predicted with just a single misclassification for each, while accurate prediction was also obtained for nine of the 10 stage III cases. Beer *et al.* (2002) recently described a prediction model, which classifies adenocarcinoma cases into high- and low-risk groups, although their model was not intended to predict 5-year survival for individual cases. The difference in 5-year survival between the high- and low-risk groups can be estimated as 40% based on the Kaplan–Meier survival curves shown in Figure 3d, whereas our nonsquamous cell carcinoma outcome classifier yielded an 81% difference in 5-year survival between the fatal and favorable classifications (Figure 5b). At present, intensive chemotherapy is given only to patients with an advanced metastatic disease. However, the development of highly accurate, individualized outcome classifiers should make it possible to select patients, who are at high risk of future failure and thus most eligible for such intensive adjuvant therapy with the intention of eradicating undetectable micrometastases, sources of future recurrence.

The gene sets used for the outcome classifiers contained various functionally relevant genes (Table 1). For example, MYC and FOSL1 are known to be involved in the process of cellular transformation (Vennstrom *et al.*, 1982; Mechta *et al.*, 1997). The MYC oncogene, frequently overexpressed with or without amplification in lung cancers, is associated with a poor prognosis (Johnson *et al.*, 1987), as is SERPINE1. (Robert *et al.*, 1999) FOSL1 has been shown to play a role as a predominant component of the AP-1 complex in ras-induced transformation (Mechta *et al.*, 1997), and it also mediates induction of SPRR1B in response to epithelial injury caused by a variety of carcinogens (Patterson *et al.*, 2001; Vuong *et al.*, 2002). Both COPB and ARCN1 constitute COPI-coated vesicles and are involved in the transport of G protein-coupled receptors, while the binding of Ras-related GTP-binding protein Cdc42 to another COPI subunit, COPG, has been shown to be important for transmitting transforming signals (Wu *et al.*, 2000). PTN and MST1 are ligands of tyrosine kinase receptors, while it has been suggested that MST1 and its receptor RON form an autocrine/paracrine system involved in cell migration of NSCLC cells (Willett *et al.*, 1998). CCT3 and ACTR3 may also be involved in motile and invasive features, since ACTR3 is a major constituent of the ARP2/3 complex required for protrusion of the lamellipodia (Craig and Chen, 2003), while CCT3 is involved in actin and tubulin folding (Martin-Benito *et al.*, 2002). Increased WEE1 expression in patients with fatal outcome may be a reflection of higher proliferative activity. In this connection, high-level expression of WEE1 in combination with the Cyclin and CDK genes has been reported in hepatocellular carcinoma (Masaki *et al.*, 2003).

Ramaswamy *et al.* (2003) recently suggested the presence of a metastatic signature based on their analysis of lung adenocarcinoma cases and identification of a 17-gene set associated with metastatic capability. It is interesting to note that two closely related genes, that is, members of the actin and small nuclear ribonucleoprotein families, are included as predictors of concordant directions in both the 12-gene set of our nonsquamous cell carcinoma outcome classifier and their 17-gene set predicting metastasis of adenocarcinomas (Tables 2 and 3). In addition to SNRPB, three other genes (EIF4A1, EIF2S2 and HNRPA1) involved in translation apparatus are also included as fatal outcome predictors in our list of top 100 genes, while

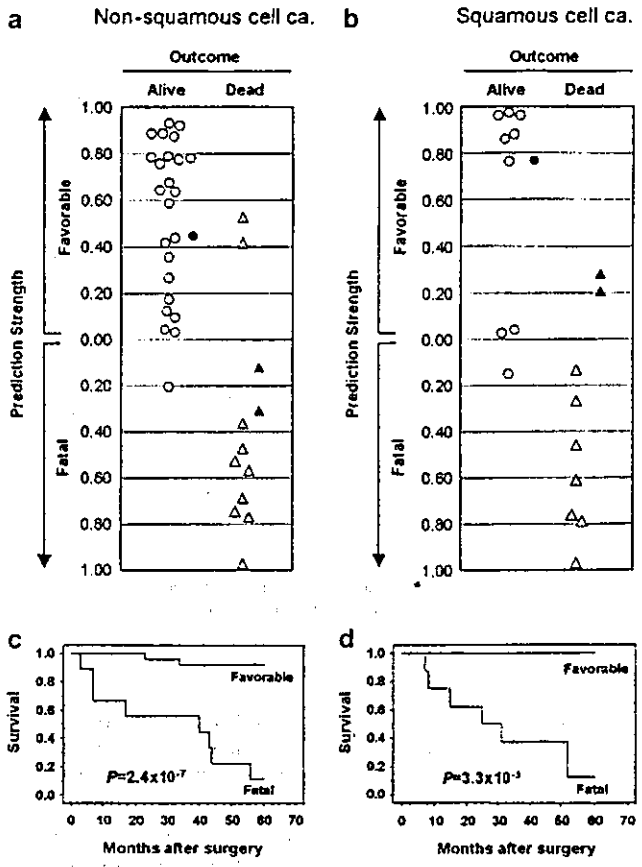

Figure 5 Results of histologic-type-specific outcome classification of nonsquamous cell and squamous cell lung cancers. The weighted-voting supervised learning was conducted using histologic-type-specific sets of genes preselected with the signal-to-noise metric. Circles and triangles indicate the same items as those in Figure 3. (a) Results for outcome classifier of nonsquamous cell lung cancer cases used for leave-one-out cross-validation (○ and △) as well as for an additional blinded validation set (• and ▲). (b) Kaplan–Meier survival curves of the 34 nonsquamous cell carcinoma cases based on the favorable and fatal outcomes predicted by the weighted-voting outcome classifier. (c) Results of outcome classification of squamous cell lung cancer cases used for leave-one-out cross-validation (○ and △) as well as for independent validation with an additional blinded sample set (• and ▲). (d) Kaplan–Meier survival curves of 16 squamous cell carcinoma cases based on the favorable and fatal outcomes predicted by the weighted-voting outcome classifier

Ramaswamy *et al.*'s 17-gene set contained two functionally related genes, EIF4EL3 and HNRPAB, suggesting the involvement of their upregulation in tumor progression. Moreover, HLA class II genes are included in both gene sets as favorable predictors. Although the use of different array platforms makes it difficult to evaluate frequencies of overlap of the selected genes in the present study and others, it is interesting that four of the five genes, which are shared by the top 100 genes of the Michigan group (Beer *et al.*, 2002) and ours, appear to be predictive in the same direction.

The outcome classifiers described here were constructed with a relatively modest number of cases, but the use of nonbiased, consecutive cases collected within a short period of time with complete follow-up data may have been a factor in their high accuracy, especially of the outcome classifier for nonsquamous cell carcinomas. This needs to be confirmed, however, in a large, independent cohort of patients, preferably in a prospective manner, before these classifiers can be put to clinical use for the selection of candidates for intensive adjuvant therapies. Nevertheless, the strategy presented here appears to be promising, and suggests that it may also be possible to develop similar predictive classifiers for predicting patients' response to conventional chemotherapy and/or molecular-targeted therapeutics such as those recently introduced involving EGF receptor inhibition. In the future, lung cancer patients who are classified as having fatal but therapeutic agent-responsive expression signatures can be expected to be selectively and intensively treated with the most appropriate active agents in an individualized manner, ultimately leading to significant improvement in the present dismal survival rate.

Our unsupervised hierarchical clustering analysis underscores previous observations that adenocarcinomas and squamous cell carcinomas are very distinct in terms of gene expression profiles (Bhattacharjee *et al.*, 2001; Garber *et al.*, 2001; Virtanen *et al.*, 2002; Kikuchi *et al.*, 2003). In addition, we observed that genes useful for constructing nonsquamous cell and squamous cell carcinoma outcome classifiers did not show any overlap, providing further support to the notion of two distinct entities. Interestingly, the unsupervised hierarchical clustering analysis used in our study demonstrated for the first time the existence of two clinically relevant subsets of squamous cell carcinomas with distinct gene expression signatures and markedly different clinicopathologic features. SQ1 showed a characteristic invasive growth pattern and a significantly worse prognosis than SQ2 (Figure 2). The most noticeable feature of the expression signature of SQ1 was high-level expression of extracellular matrix proteins, including fibronectin, SPARC and various collagen subunits such as α2(I) and α1(III) (Figure 1f). By using an expression profiling analysis of a *in vivo*-selected, highly metastatic melanoma model, Clark *et al.* (2000) found that enhanced expression of genes involved in the extracellular matrix assembly, including fibronectin, collagen α2(I) and α1(III), was associated with the acquisition of a metastatic phenotype during the *in vivo* selection, a finding consistent with the invasive growth pattern and poor prognosis of SQ1 in our study. Ramaswamy *et al.* (2003) also found a similar association between metastatic potential and collagen gene expression in the molecular signature analysis of solid tumors. In addition, expression of a set of ESTs was found to be distinctly reduced in SQ1 when compared with SQ2 (Figure 1c), suggesting that the reduced expression of genes corresponding to these ESTs may be related to the aggressive nature of SQ1. Although the gene expression-based subclasses of squamous cell carcinomas were identified by using a small cohort of squamous cell carcinomas, the present findings warrant further validation and characterization.

In view of their distinct molecular signatures, the existence of a few subclasses of adenocarcinomas has been reported (Bhattacharjee *et al.*, 2001; Garber *et al.*, 2001; Beer *et al.*, 2002; Virtanen *et al.*, 2002), although the expression signatures identified in these studies did not show complete correspondence with each other or with those identified by us. However, there is a high degree of consistency in the fact that all these studies have identified a subset of adenocarcinomas with a high-level expression of genes related to differentiation of normal peripheral lung epithelial cells such as TTF-1 and SP-C. This subclass of adenocarcinomas is most typically represented by AD3 in our study, which appears to correspond to AD group 2 in the Stanford study and to C4 in the MIT study. Consistently notable features of this subclass are significantly higher proportions of females, non/light smokers and well-differentiated tumors. These findings are consistent with our previous observations that there is a subset of adenocarcinomas which may represent those arising from cells committed to become peripheral lung epithelial cells under weaker influence of smoking (Yatabe *et al.*, 2002).

In conclusion, we have been successfully constructing an individualized outcome prediction classifier, which appears to be useful especially for nonsquamous cell carcinomas. In addition, we have been able to demonstrate the presence of marked heterogeneities of NSCLCs by identifying clinically relevant subclasses not only for adenocarcinomas but also for squamous cell carcinomas. Further studies appear to be warranted on the basis of these findings, with the aim to improve both understanding and survival of this fatal disease.

Materials and methods

Tissue sample

A total of 50 NSCLC tissue specimens (30 adenocarcinomas, 16 squamous cell carcinomas and four large cell carcinomas) were obtained from 15 female and 35 male patients, who had consecutively undergone potentially curative resection at Aichi Cancer Center Hospital (Nagoya, Japan). The vast majority of these lung cancer specimens were acquired within an 11-month period between December 1995 and October 1996, while squamous cell and large cell carcinomas were also obtained during an additional few months around this period of time. An additional three cases each of adenocarcinomas and squamous cell carcinomas, which were collected just before or after the specimen collection period, were used for an independent validation dataset. The tumor specimens were embedded in OCT compound and stored at −80°C until use with the approval of the institutional review board. The median age of this cohort was 63 (range: 43–76), and there were 23 pStage I tumors, 11 pStage II, and 16 pStage III. Approvals for this study were obtained from the institutional review board of the Aichi Cancer Center.

RNA extraction and microdissection

On average, 50 7 μm-thick cryostat sections were prepared for the extraction of total RNA from tumor cell-rich areas, which were identified by a surgical pathologist (YY) using every 10th section stained by May–Giemsa. Careful attention was paid to the microdissection of only such tumor cell-rich areas, yielding an average of 75.4% tumor cell content (Figure 1i). RNAs were then isolated using RNAeasy (Quiagen, Valencia, CA, USA) according to the manufacturer's instruction, and their quality was checked with the RNA 6000 Nano Assay kit and the 2100 Bioanalyzer (Agilent, Palo Alto, CA, USA).

Microarray experiments and acquisition of datasets

We used two sets of membrane cDNA microarrays (GeneFilter Human Microarrays Release I and Release II; Invitrogen, Carlsbad, CA, USA), which contained a total of 11 168 spots corresponding to 8644 independent genes. A measure of 5 μg of total RNA was reverse-transcribed using oligo-dT primers (Invitrogen) and SuperScript II reverse transcriptase (Invitrogen) in the presence of 100 μCi of [^{33}P]dCTP (Amersham Bioscience, Piscataway, NJ, USA) according to the instructions for the GeneFilters (Invitrogen) with slight modification. The GeneFilters were prehybridized for 2 h at 51°C with 0.5 μg/ml of poly-dA (Invitrogen) and 0.5 μg/ml Cot-1 DNA (Invitrogen) in 10 ml of AlkPhos DIRECT hybridization buffer (Amersham Bioscience) and then hybridized for 17 h at 51°C with the denatured radiolabeled probe. Hybridization of the arrays was followed by two washings with a solution containing 2 M of urea, 0.1 % of SDS, 50 mM of Na phosphate buffer (pH 7.0), 150 mM of NaCl, 1 mM of $MgCl_2$ and 0.2% of AlkPhos DIRECT blocking reagent (Amersham Bioscience). The arrays were then washed twice with a solution containing 2 mM of $MgCl_2$, 50 mM of Tris and 100 mM of NaCl, and with a solution containing 2 mM of $MgCl_2$, 50 mM of Tris and 15 mM of NaCl. All procedures were carried out with the aid of custom-made AutoHybridizers (Fuji Photo Film, Tokyo, Japan). The arrays were then exposed for 2 h to an Imaging Plate and scanned at 25-μm resolution with a BAS5000 phosphoimager (Fuji Photo Film), images of the hybridized arrays were processed with L Process (Fuji Photo Film) and signal intensities quantified with ArrayGauge software (Fuji Photo Film). After each hybridization, the arrays were stripped by boiling them in 0.5% SDS solution for 60 min and scanned for residual hybridization before the next round of hybridization with a newly labeled probe of the same sample to acquire their expression profiles in duplicate.

Data rescaling and preprocessing

The raw data were rescaled to account for the differences in individual hybridization intensities. We employed a rank-invariant scaling method to select genes (Tseng *et al.*, 2001), which were then used for fitting of a nonlinear normalization curve. After normalization, scatter plots of the 50 pairs of replicate data points for each of the genes were generated, the reproducibility of expression between the replicate pairs was assessed, and genes showing a Pearson correlation coefficient higher than 0.85 were selected. Averaged values of the first and the second hybridizations were used for further analyses. In addition, genes whose expression levels did not vary by a factor of at least 2 across the 50 samples were eliminated, because they were unlikely to be informative. Genes with a median intensity lower than 0.3 were also filtered out from the following analyses.

Hierarchical clustering and construction of outcome classifiers

Average linkage hierarchical clustering was performed by using the Cluster program following log transformation and median centering, and the results were visualized using the TreeView program (Eisen *et al.*, 1998). Predictive genes that most effectively distinguished prognosis-favorable patients